Turbulent particle-gas suspensions

V. Kumaran & P. S. Goswami

Department of Chemical Engineering
Indian Institute of Science

Practical applications:

- Atmospheric aerosols, dust storms.
- Pneumatic transport of solids.
- Fluidized & circulating beds.
- Clean coal separation.
- Cyclone separator.

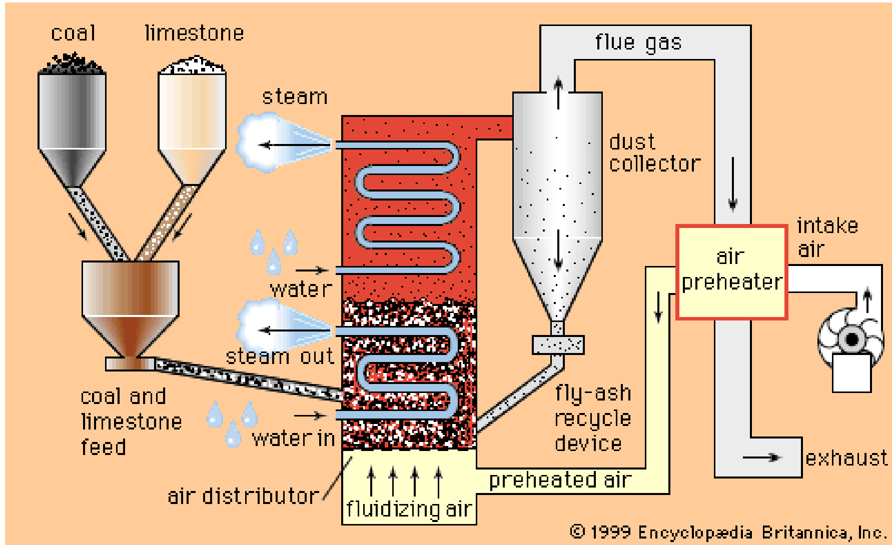

Gas-particle suspensions:

Colloidal $d < 1\mu$ m:

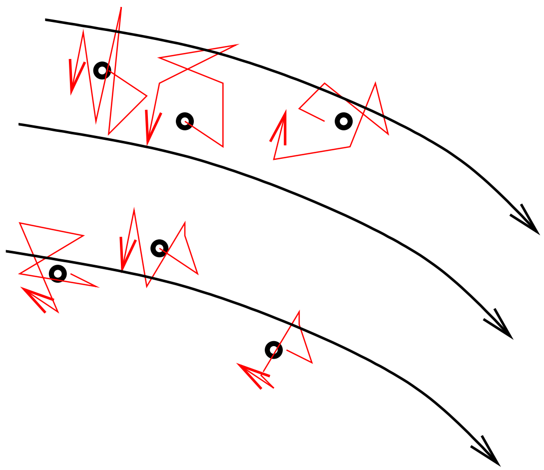

Aerosol 1μ m $< d < 10\mu$ m:

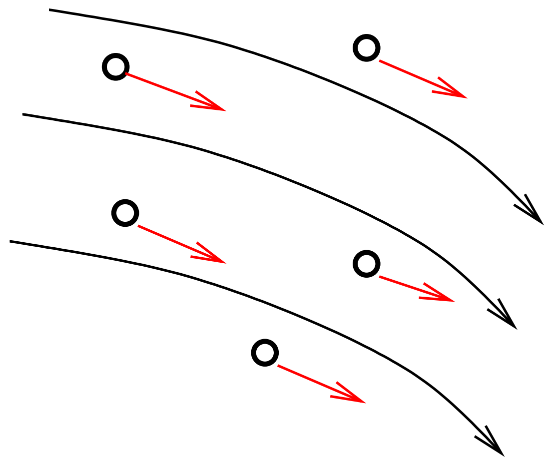

Suspension $10\mu\text{m} < d < 100\mu$ m:

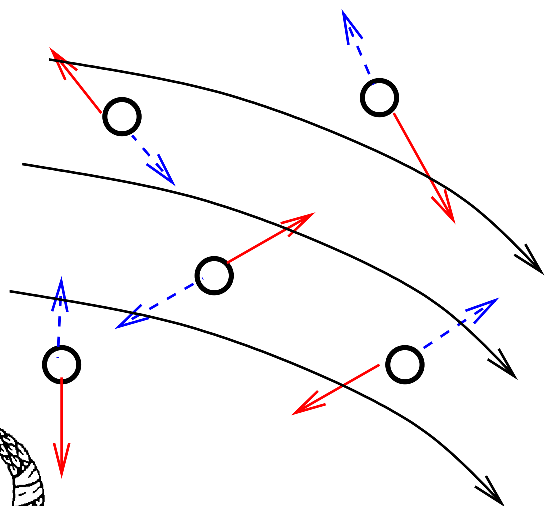

Granular material $d > 100\mu$ m:

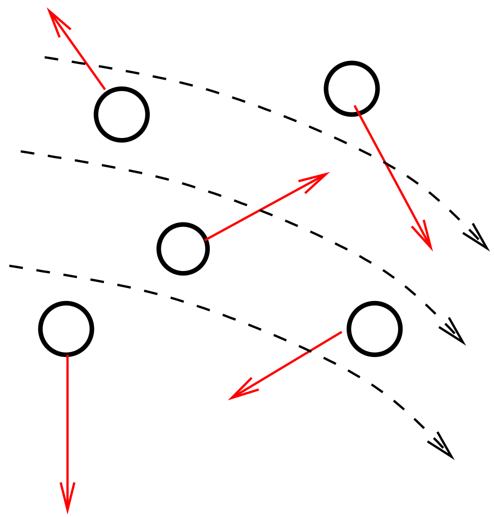

Gas-particle suspensions:

Parameters:

- Terminal velocity $U_t = (mg/3\pi\mu d) \sim d^2$.
- Brownian diffusivity $D_B = (k_B T/3\pi\mu d) \sim d^{-1}$.
- Peclet number (convection/Brownian diffusion)
  Pe = $(U_t d/D_B) \sim d^{-4}$.
- Reynolds number (fluid inertia/fluid viscosity)
  Re = $(\rho_g U_t d/\mu) \sim d^3$.
- Stokes number (particle inertia/fluid viscosity)
  St = $(\rho_p U_t d/\mu) \sim d^3$.

$\rho_g = 1 kg/m^3$, $\rho_p = 10^3 kg/m^3$, $\mu = 1.8 \times 10^{-5} kg/m/s$,
$T = 300K$.

Gas-particle suspensions:

Colloidal $d < 1\mu$ m:

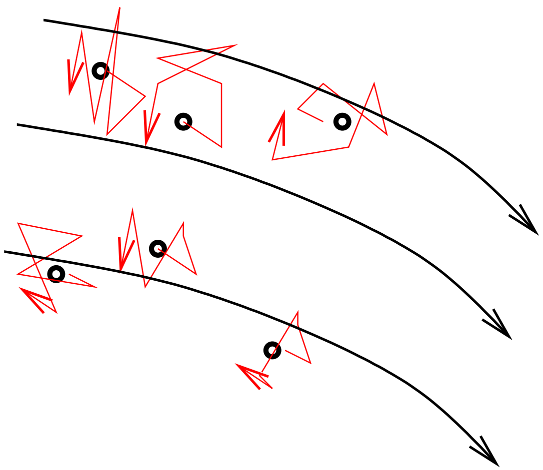

$U_t < 1.5 \times 10^{-5}$.

$D_B > 1.2 \times 10^{-11}$.

$(U_t d / D_B) < 1.3$.

Reynolds number $Re < 8.5 \times 10^{-7} >$.

Stokes number $St < 8.5 \times 10^{-4}$.

Fluid viscosity dominant.

Gas-particle suspensions:

$$1.5 \times 10^{-5} < U_t < 1.5 \times 10^{-3}.$$

$$1.2 \times 10^{-11} < D_B < 1.2 \times 10^{-12}.$$

$$1.3 < (U_t d/D_B) < 1.3 \times 10^4.$$

Aerosol 1μ m $< d < 10\mu$ m:

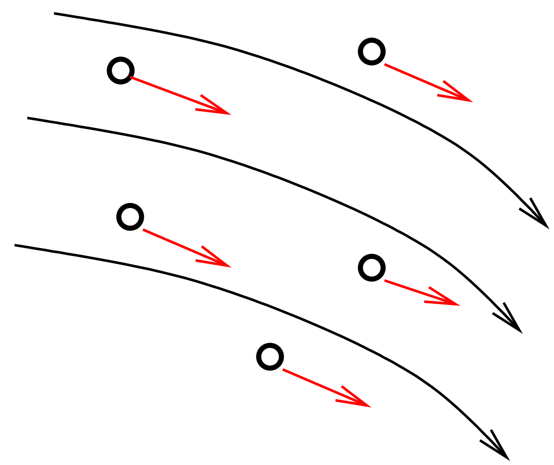

Reynolds number $8.5 \times 10^{-7} Re < 8.5 \times 10^{-4} >$.

Stokes number $8.5 \times 10^{-4} < St < 8.5 \times 10^{-1}$.

Fluid viscosity dominant.

Gas-particle suspensions:

$1.5 \times 10^{-5} < U_t < 1.5 \times 10^{-3} m/s$

$1.2 \times 10^{-11} < D_B < 1.2 \times 10^{-12}$.

$1.3 \times 10^4 < (U_t d/D_B) < 1.3 \times 10^8$.

$8.5 \times 10^{-4} <$ **Re** $< 8.5 \times 10^{-1}$.

$8.5 \times 10^{-1} <$ **St** $< 8.5 \times 10^{2}$.

Suspension 10μm $< d < 100\mu$ m:

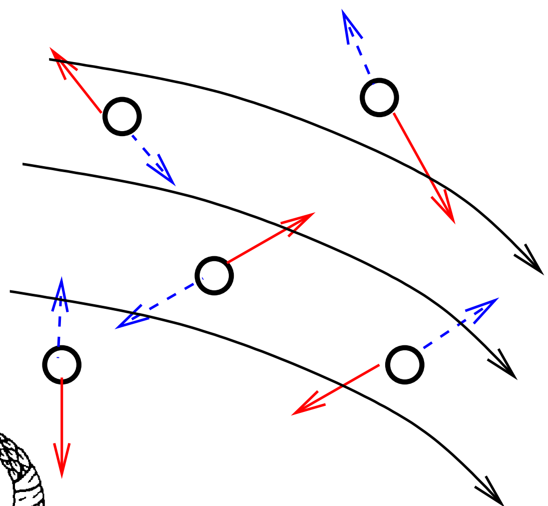

Balance:
Particle inertia vs.
Fluid viscosity

Gas-particle suspensions:

$1.5 \times 10^{-3} < U_t < 1.5 \times 10^{-1}$

$1.2 \times 10^{-12} < D_B < 1.2 \times 10^{-13}$.

$1.3 \times 10^{8} < (U_t d/D_B) < 1.3 \times 10^{12}$.

$8.5 \times 10^{-1} < \mathbf{Re} < 8.5 \times 10^{2}$.

$8.5 \times 10^{2} < \mathbf{St} < 8.5 \times 10^{5}$.

Fluid viscosity negligible.
Dominated by particle inertia & contact dissipation.

Granular material $d > 100\mu$ m:

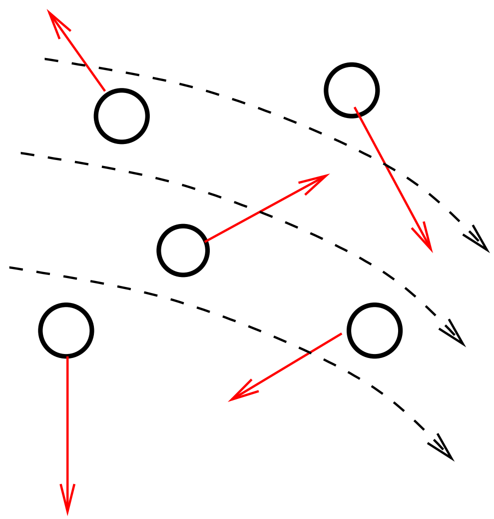

Gas-particle suspensions:

Colloidal $d < 1\mu$ m:

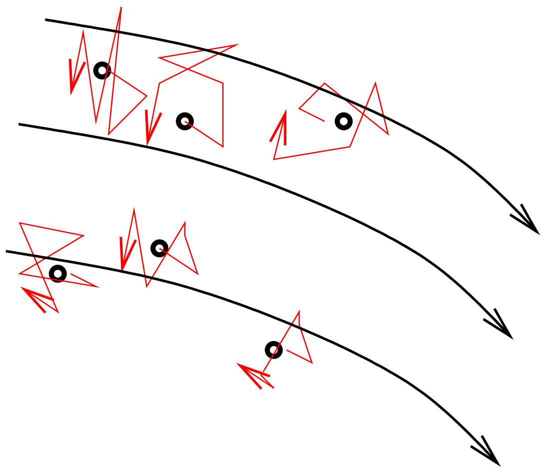

Aerosol 1μ m $< d < 10\mu$ m:

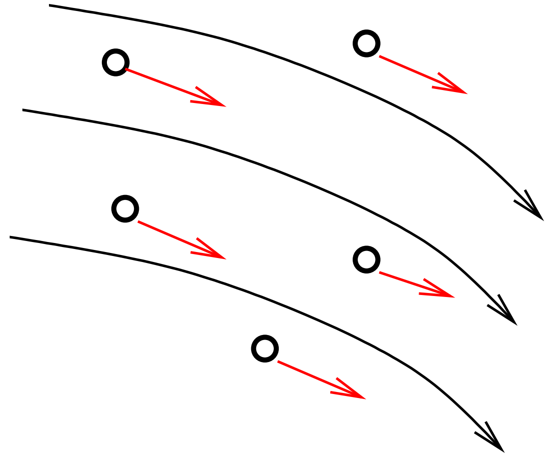

Suspension 10μm $< d < 100\mu$ m:

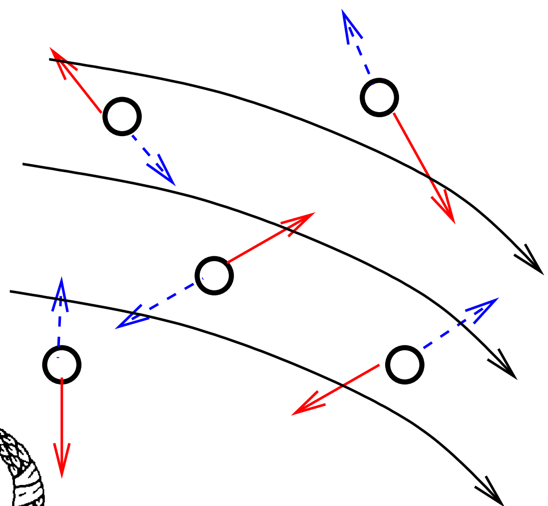

Granular material $d > 100\mu$ m:

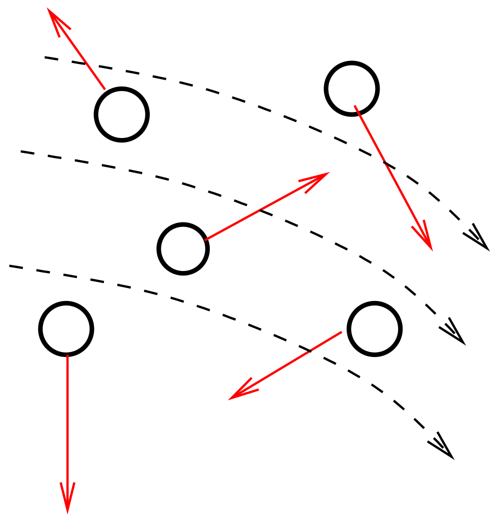

Gas-particle suspensions:

Colloidal $d < 1\mu$ m:

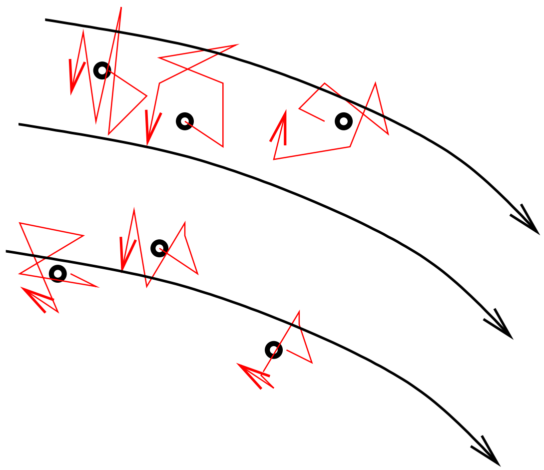

Aerosol 1μ m $< d < 10\mu$ m:

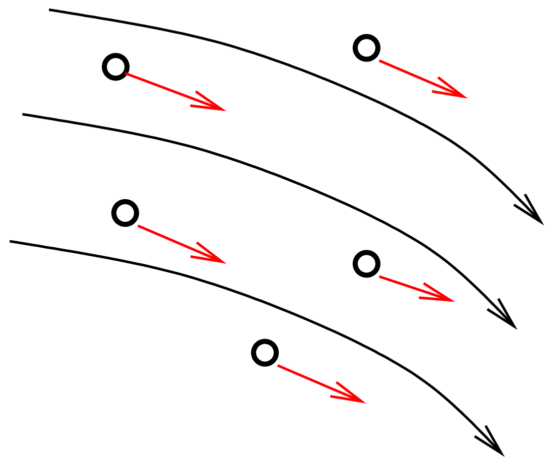

Suspension $10\mu\text{m} < d < 100\mu$ m:

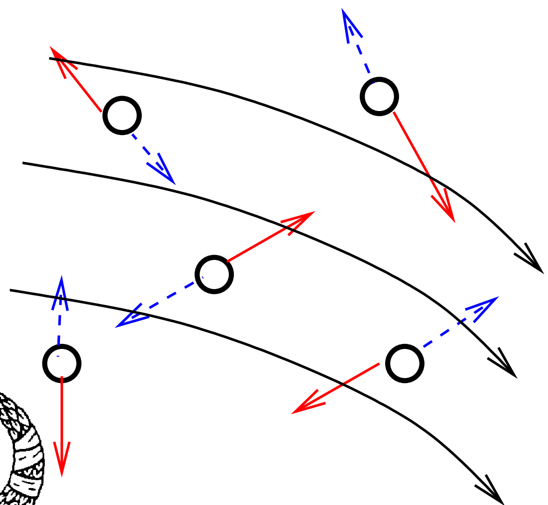

Granular material $d > 100\mu$ m:

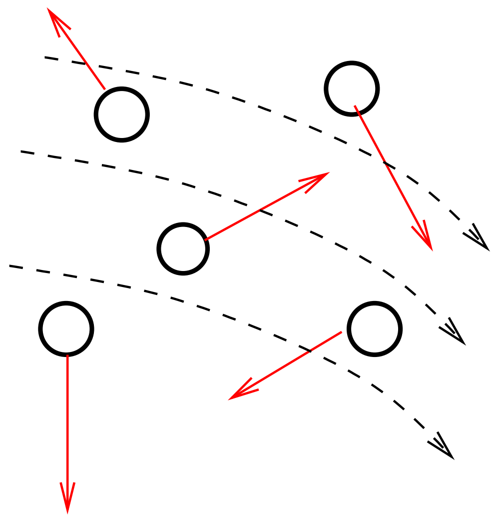

Turbulent particle-gas suspensions:

Current ‘two-fluid’ models treat particle & fluid as two continuous phases, and write equations for the average density and velocities.
Particle phase:

$$\frac{\partial \rho_p}{\partial t} + \nabla . \mathbf{u}_p = 0$$

$$\rho(\partial_t \mathbf{u}_p + \mathbf{u}_p . \nabla \mathbf{u}_p) = -\nabla p_p + \eta_p \nabla^2 \mathbf{u}_p + \mathbf{f}_f$$

Disadvantage:

Local rates of heat and mass transfer proportional to *local relative velocity between particle and fluid*, and not the man velocity difference.

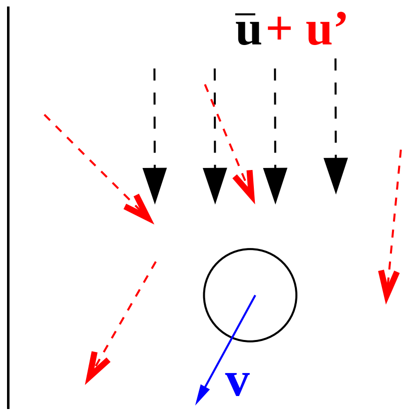

Turbulent particle-gas suspensions:

Current 'two-fluid' models treat particle & fluid as two continuous phases, and write equations for the average density and velocities. Particle phase:

$$\frac{\partial \rho_p}{\partial t} + \nabla . \mathbf{u}_p = 0$$

$$\rho(\partial_t \mathbf{u}_p + \mathbf{u}_p . \nabla \mathbf{u}_p) = -\nabla p_p + \eta_p \nabla^2 \mathbf{u}_p + \mathbf{f}_f$$

Objective — take account of fluctuations in realistic way.

- Particle velocity distribution.
- Effect of turbulent fluid velocity fluctuations on particle phase.
- Effect of particle velocity fluctuations on fluid turbulence.

Outline:

Turbulent particle-gas suspension with particle Reynolds number $Re < 10$, particle Stokes number $St > 1000$:

- Microscopic model for particle phase.
- Comparison with simulations/experiments.
- Incorporating turbulent fluctuations in continuum model.

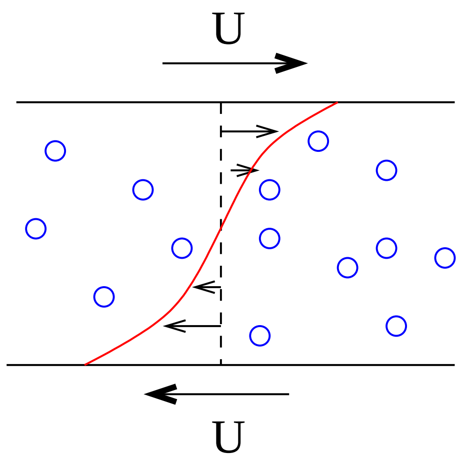

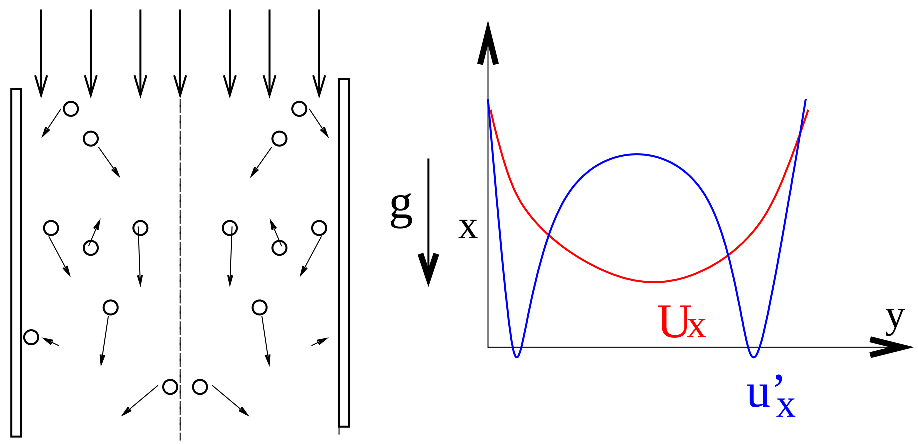

Turbulent gas-particle suspensions:

Particle dynamics:

$$m \frac{d\mathbf{u}_i}{dt} = \sum_i \mathbf{F}_i$$

- Drag force.
- Inter-particle collisions.
- Buoyancy force.
- Lift force.
- Virtual mass effect.
- Basset force.
- ...

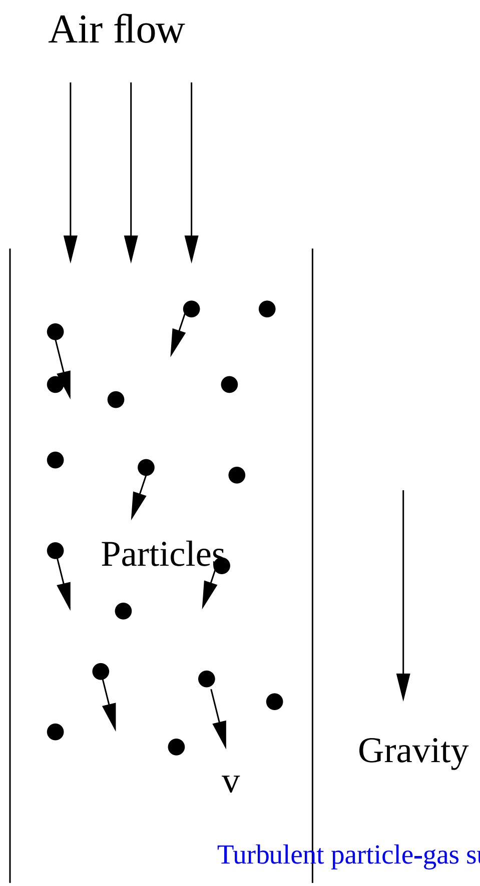

Turbulent gas-particle suspensions:

Particle Reynolds number $Re < 10$:
Particle Stokes number $St > 1000$:

- Drag force.
- Inter-particle collisions.
- Buoyancy force.
- Lift force.
- Virtual mass effect.
- Basset force.
- ...

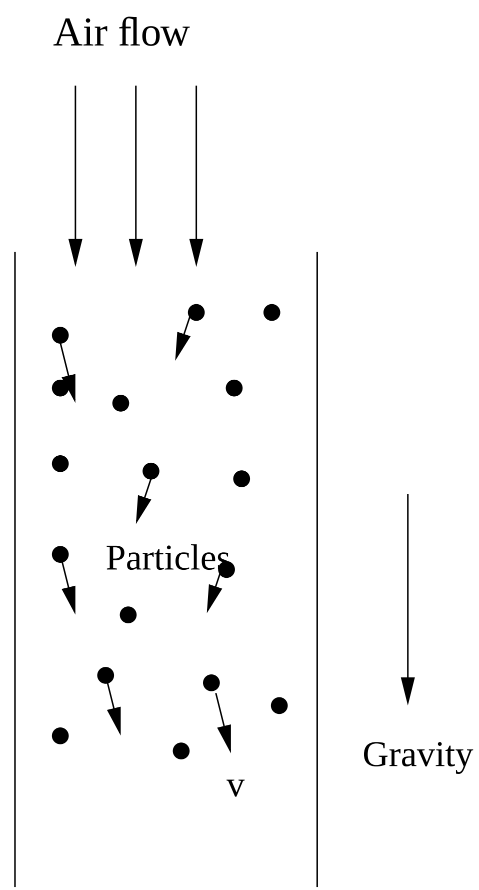

Schematic of particle laden flow.

Turbulent gas-particle suspensions:

Particle drag force: Re < 10:

$$\mathbf{a} \;=\; \frac{\mathbf{u} - \mathbf{v}}{\tau_v}$$

Viscous relaxation time:
Stokes law:

$$\tau_v = (\rho d^2/18\mu)$$

Inertial correction:

$$\tau_v = \frac{\rho d^2}{18\mu(1 + 0.15 Re^{0.687})}$$

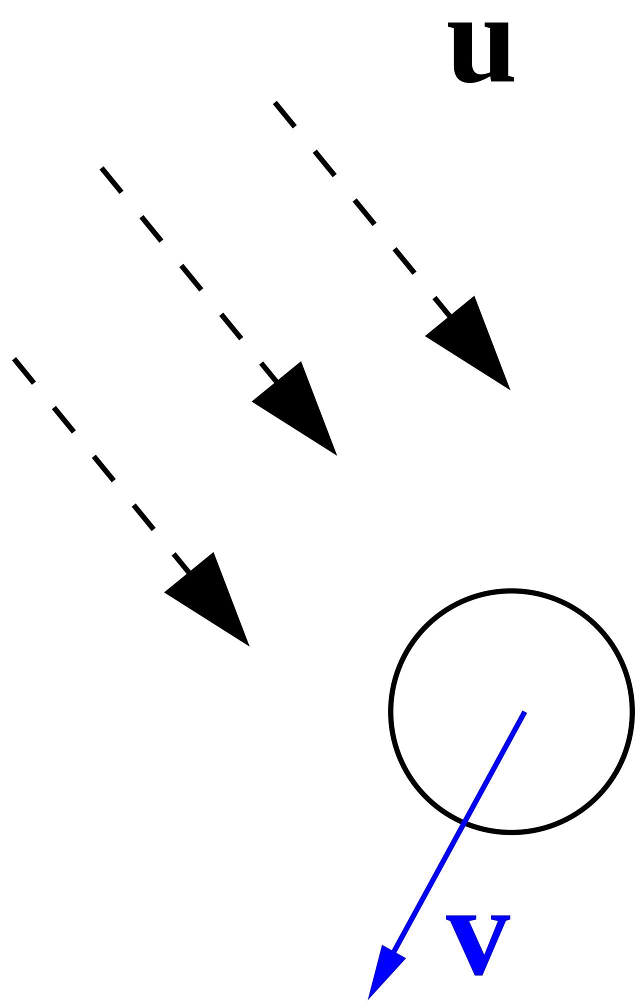

Turbulent particle-gas suspensions:

Time scales:

Fluid integral time τ_f

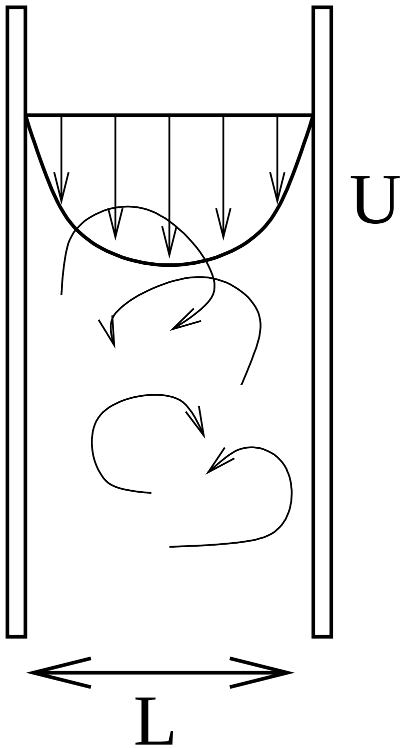

$\tau_f \sim (L/u)$

Particle relaxation time τ_p

$\tau_p = (3\pi\eta d/m)$

$\tau_p = (\rho_p d^2/18\eta)$

Particle collision time τ_c

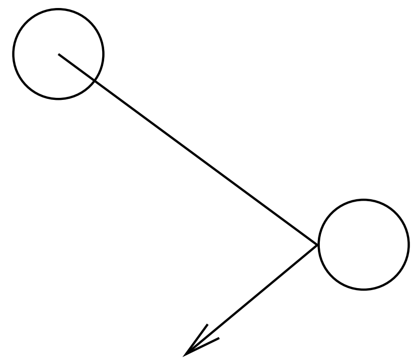

$\tau_c = 1/(nd^2 v)$

$\tau_c = (\pi\rho_s d/6v\text{vol fr})$

Simulation technique:

- Direct numerical simulations.
- Particle event-driven simulations.

$$m\frac{d\mathbf{u}_i}{dt} = \sum_i \mathbf{F}_i$$

Simulation advances in discrete time steps.

Flow equations

Navier-Stokes equation for fluid phase:

$$
\begin{aligned}
\nabla \cdot \mathbf{u}_i &= 0 \\
\frac{\partial \mathbf{u}_i}{\partial t} + \mathbf{u}_i \cdot \nabla \mathbf{u}_i &= -\frac{1}{\rho} \nabla p_i + \nu \nabla^2 \mathbf{u}_i
\end{aligned}
$$

Particle phase equation:

$$
\begin{aligned}
\frac{d\mathbf{v}_i}{dt} &= \frac{\mathbf{u}_i\left(\mathbf{x}_{Pi}\right) - \mathbf{v_i}}{\tau_v} + \frac{1}{m_p} \sum_{i \neq j} \mathbf{F}_{ij} \\
\frac{d\mathbf{x}_i}{dt} &= \mathbf{v}_i
\end{aligned}
$$

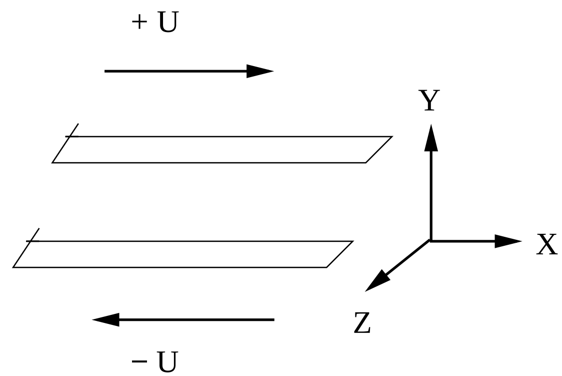

Schematic of particle laden flow.

Validation of DNS: Couette flow.

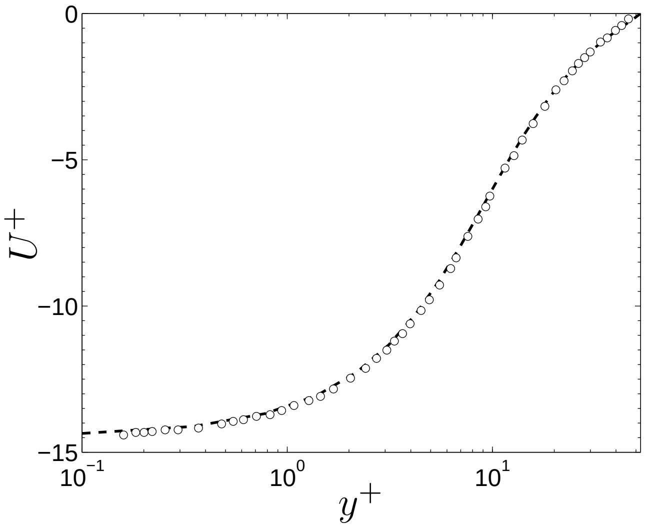

Mean velocity profile

present simulation (−−) and Komminaho et al. (1996) (∘)

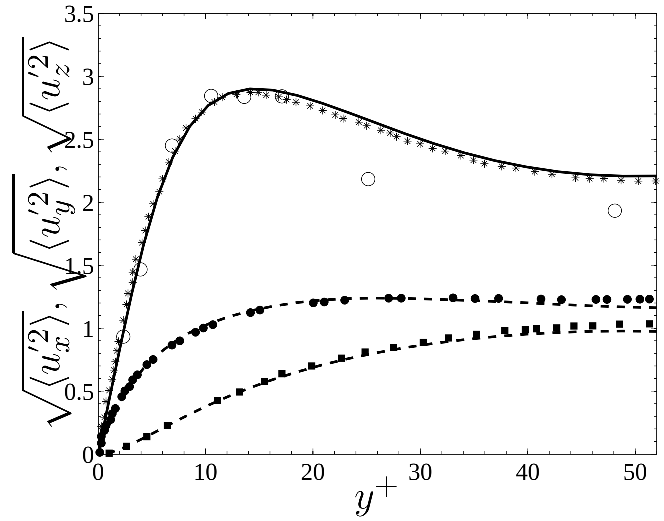

Root mean square velocity fluctuation $\sqrt{\langle u_x'^2\rangle}$, Komminaho et al. (1996) ($*$); $\sqrt{\langle u_z'^2\rangle}$,Komminaho et al. (1996) (●); $\sqrt{\langle u_y'^2\rangle}$ Komminaho et al. (1996) (■); $\sqrt{\langle u_x'^2\rangle}$ present (—), $\sqrt{\langle u_z'^2\rangle}$, present (−−); $\sqrt{\langle u_y'^2\rangle}$ present,(−.−); $\sqrt{\langle u_x'^2\rangle}$ Bech et. al. (∘)

Validation of DNS: Channel flow.

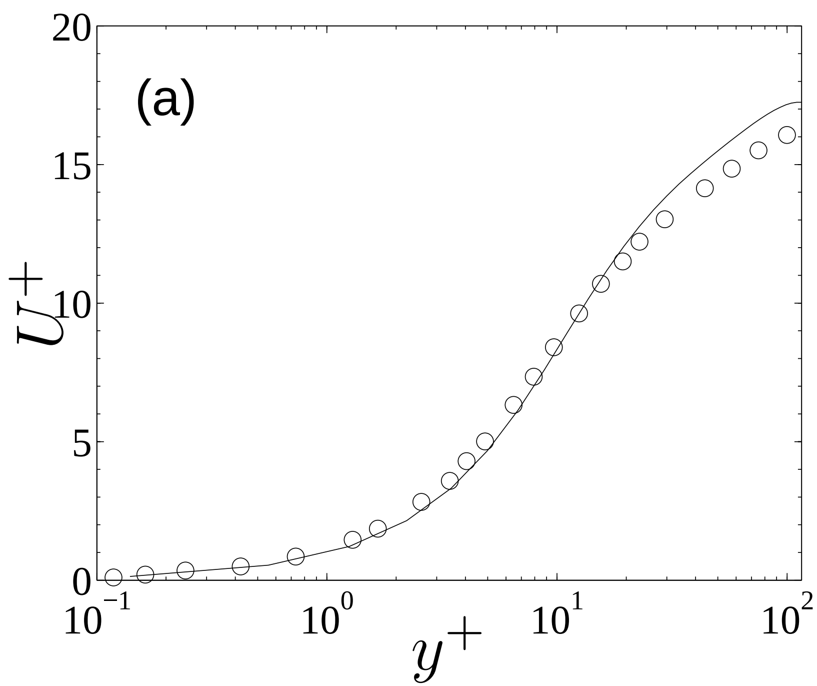

Air mean velocity; Re_c=1994

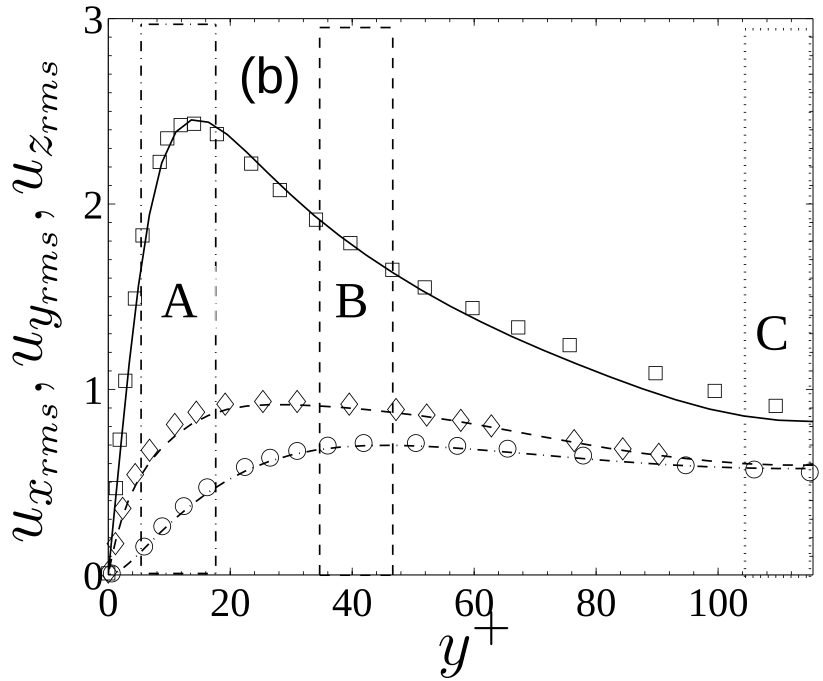

Gas-phase root-mean-square velocity fluctuation

(—) is obtained from our simulation at $Re_\tau = 115.5$,

(○) is from Mclaughlin(2001) at $Re_\tau = 125$.

$u_{x_{rms}}$ (—); $u_{y_{rms}}$ (-.-); $u_{z_{rms}}$ (–) are obtained from present DNS,

$u_{x_{rms}}$ (□); $u_{y_{rms}}$ (○); $u_{z_{rms}}$ (◇), obtained from Mclaughlin (2001).

Turbulent particle-gas suspensions:

1. Fluid autocorrelation time small compared to particle relaxation & collision time.
2. Force due to fluid velocity decorrelates over time taken for particle to relax.
3. Consider force due to fluid as a delta function correlation in time.

$$\langle \mathbf{f}(t)\mathbf{f}(t')\rangle = \mathbf{D}(\mathbf{x})\delta(t-t')$$

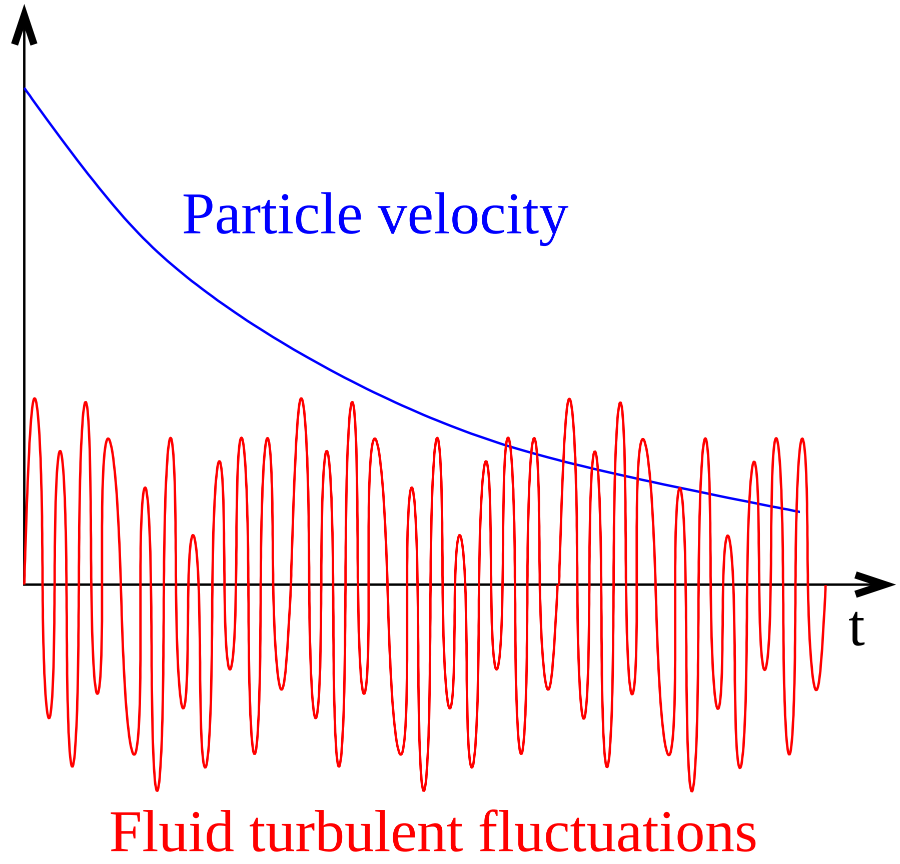

Fluctuating force model:

Based on Brownian motion:

- Force on Brownian particle due to forces exerted by molecules in a liquid.
- Correlation time of force small compared to particle relaxation time.
-

$$\langle \xi(t)\xi(t')\rangle = A\delta(t-t')$$

- Gaussian distribution for force components.

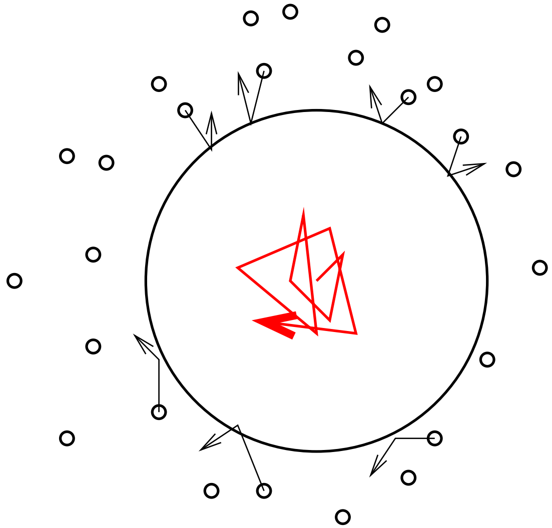

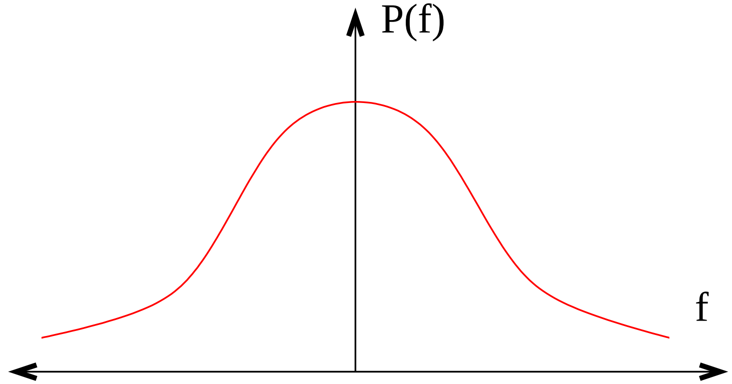

Brownian motion:

Langevin equation:

$$m\frac{du}{dt} = -3\pi\mu d u + \xi$$

$$\langle u^2\rangle = \frac{2}{\tau_v}\langle \xi^2\rangle = \frac{k_B T}{2m}$$

$$\langle \xi^2\rangle = \frac{k_B T}{m\tau_v}$$

$$\langle x^2\rangle = \frac{2k_B T}{3\pi\mu d}$$

Diffusion equation:

$$\frac{\partial\rho}{\partial t} = D\frac{\partial^2\rho}{\partial x^2}$$

$$\rho(x, t=0) = \delta(x - x_0)$$

$$\rho = (4\pi D t)^{-1/2}\exp\left(-x^2/4Dt\right)$$

$$\langle x^2\rangle = \int_0^\infty dx(x^2\rho(x)) = 2Dt$$

Stokes-Einstein relation: $D = (k_B T/3\pi\mu d)$.

Fluctuating force model:

- Particle acceleration — fluid mean and fluctuating velocity.

$$\mathbf{a} = \frac{\mathbf{u} - \mathbf{v}}{\tau_v}$$

$$\mathbf{a} = \frac{\bar{\mathbf{u}} - \mathbf{v}}{\tau_v} + \frac{\mathbf{u}'}{\tau_v}$$

- Fluctuating part $(\mathbf{u}'/\tau_v)$ as Brownian force.

$$m\frac{d\mathbf{v}}{dt} = \frac{(\bar{\mathbf{u}} - \mathbf{v})}{\tau_v} + \mathbf{f}$$

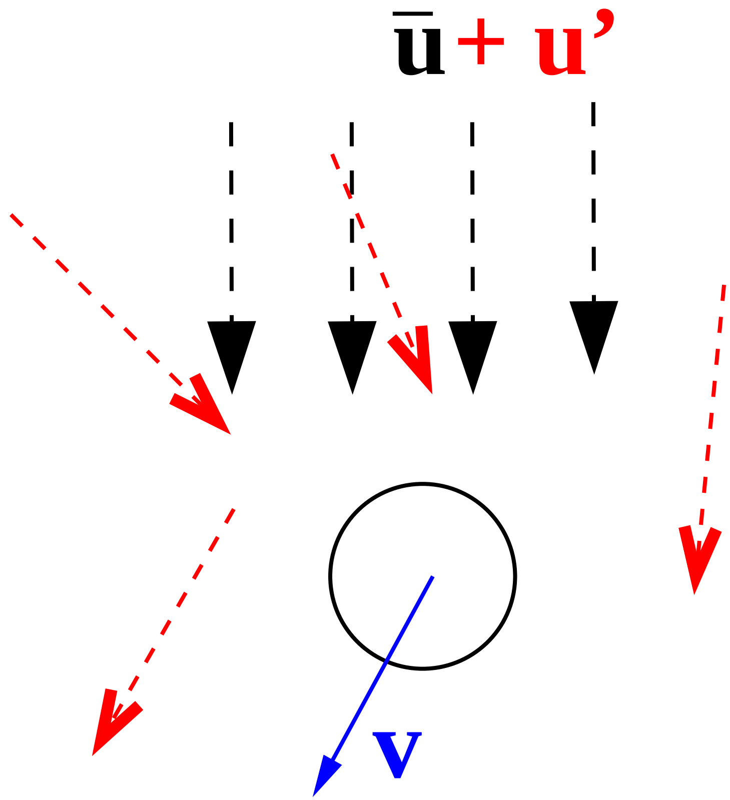

Fluctuating force: Similarities to Brownian motion.

Fluid velocity fluctuations — near Gaussian?

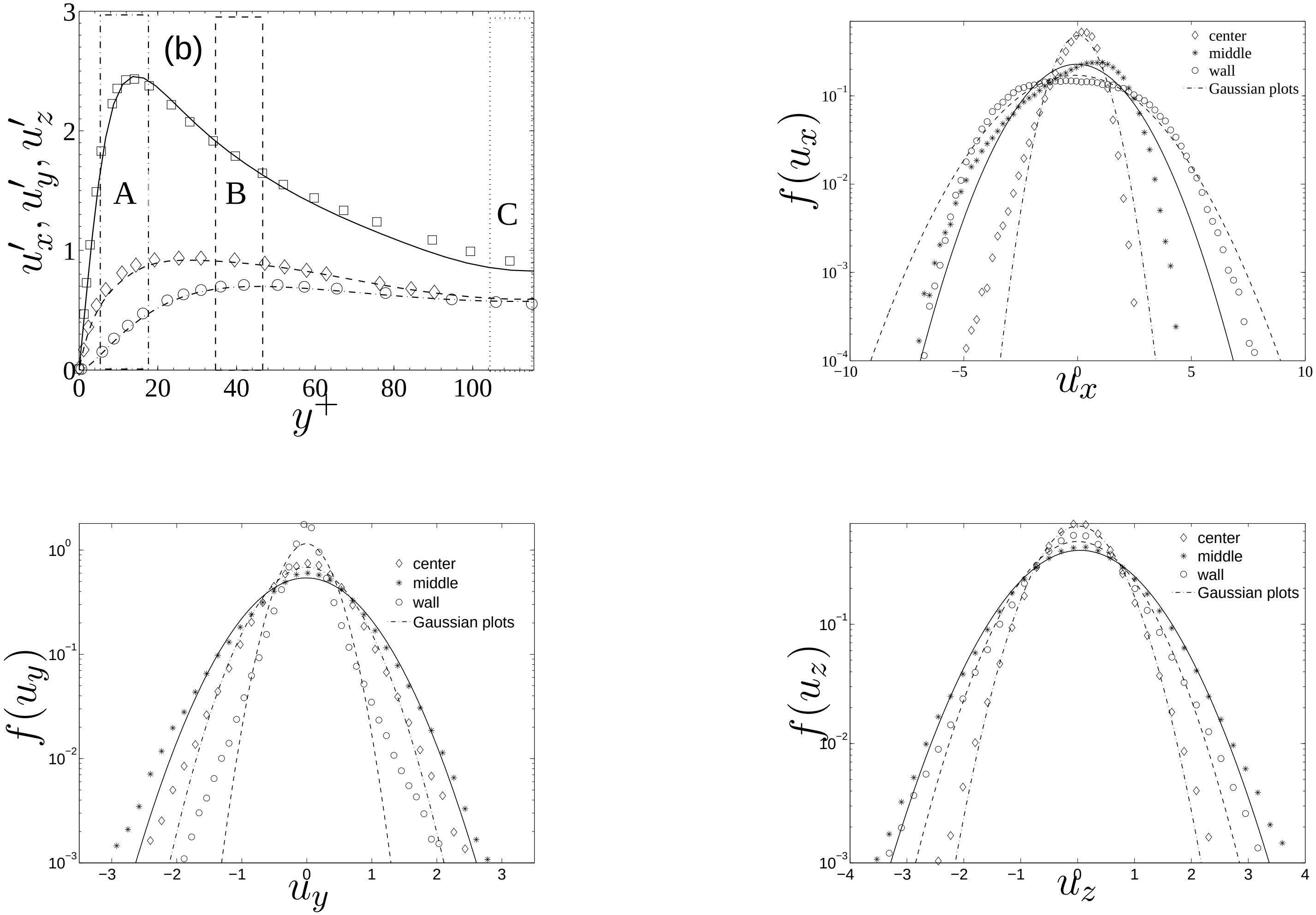

$\circ$ Region A, $*$ Region B, $\diamond$ Region C.

Fluctuating force: Similarities to Brownian motion.

Fluid correlation time short? Decorrelation times in different reference frames.

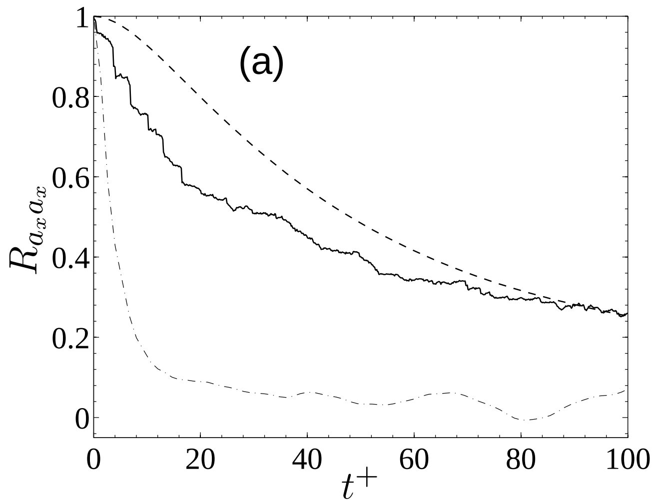

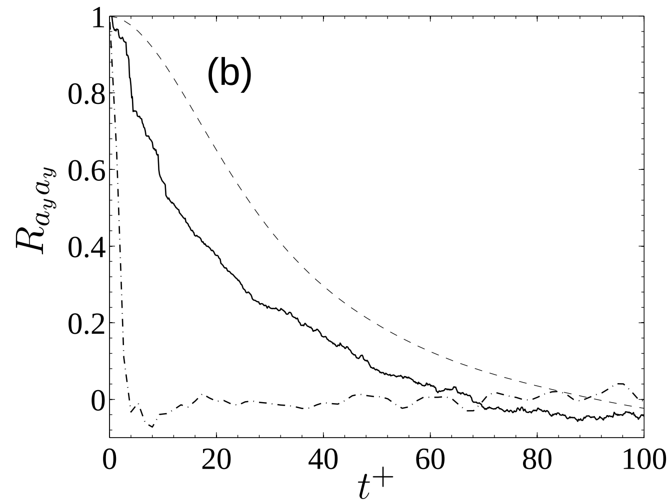

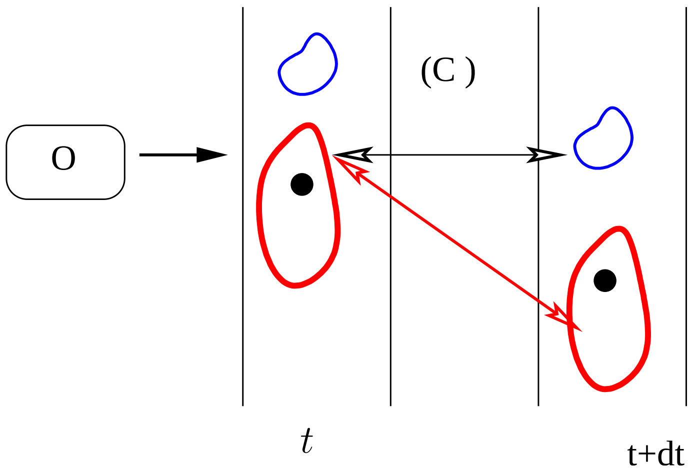

(a) Stream-wise, (b) wall-normal

Fixed Eulerian frame (—.—),

Moving Eulerian frame (— —), Particle

acceleration correlation (—)

Fluctuating force model:

Differences from Brownian motion:

- Noise anisotropic.

$$\langle f_x^2 \rangle \neq \langle f_y^2 \rangle \neq \langle f_z^2 \rangle \neq$$

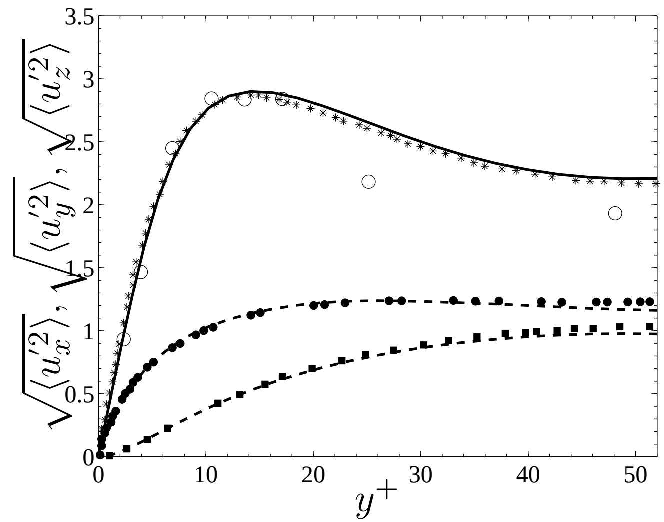

- Spatially inhomogeneous.
- Cross-correlation.

$$\langle f_x f_y \rangle \neq 0$$

Fluctuating force: Similarities to Brownian motion.

Lack of correlation between particle concentration and fluid velocity fluctuations?

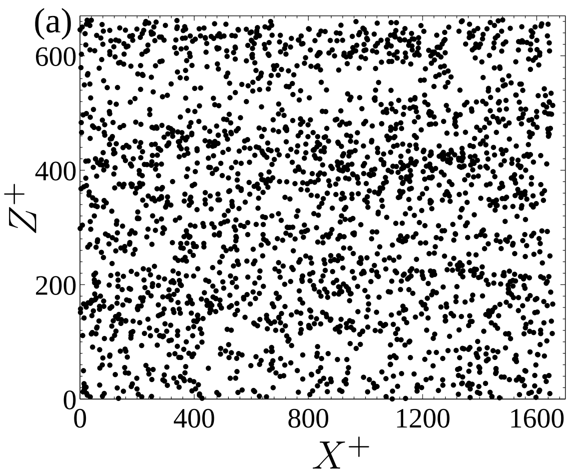

$\tau_v = 24.2$

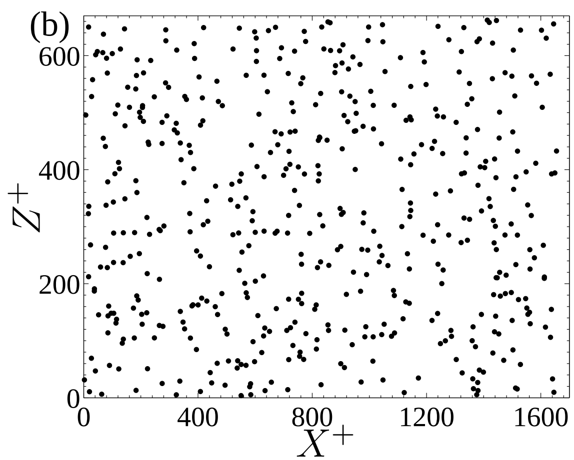

$\tau_v = 193.9$

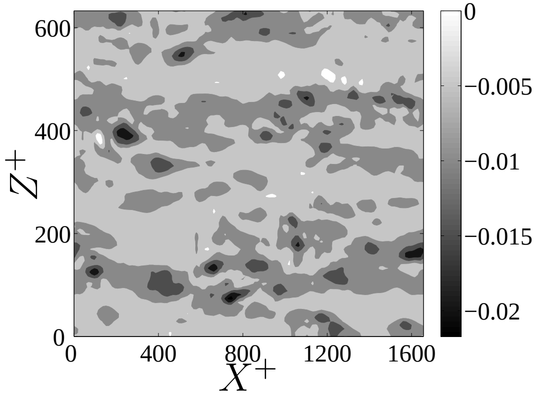

Fluctuating force simulations:

Langevin equation:

$$\frac{d\mathbf{v}}{dt} = -\frac{(\mathbf{v} - \bar{\mathbf{u}})}{\tau_v} + \mathbf{F}(t)$$

Equivalent Fokker-Planck equation:

$$\frac{\partial f\left(\mathbf{v}'\right)}{\partial t} = \frac{1}{\tau_v}\frac{\partial (v_i' f(\mathbf{v}'))}{\partial v_i'} + D_{ij}\frac{\partial^2 f\left(\mathbf{v}'\right)}{\partial v_i' \partial v_j'}.$$

Noise correlations: $\langle F_i(t) F_j(t) \rangle = 2 D_{ij} \delta(t - t'),$
Difference equation for velocity:

$$v_i(t + \Delta t) - v_i(t) = -\frac{(v_i - \bar{u}_i)\Delta t}{\tau_v} + F_i \Delta t$$

Fluctuating force simulations:

Force calculation: Two random numbers ζ_1, ζ_2.

$$F_x = \frac{\sqrt{2D_{xx}}\zeta_1}{\sqrt{\Delta t}}$$

$$F_y = \frac{\sqrt{2D_{yy}}}{\sqrt{\Delta t}} \left(\frac{D_{xy}\zeta_1}{\sqrt{D_{xx}D_{yy}}} + \zeta_2 \sqrt{1 - \frac{D_{xy}^2}{D_{xx}D_{yy}}} \right)$$

Diffusion coefficient:

$$D_{ij} = \frac{\langle u'_i(0)u'_j(0)\rangle}{\tau_v^2} \int_0^\infty dt' \frac{\langle u'_i(t')u'_j(0)\rangle}{\langle u'_i(0)u'_j(0)\rangle}$$

$$= \frac{\langle u'_i(0)u'_j(0)\rangle}{\tau_v^2} \int_0^\infty dt' R_{ij}.$$

Diffusion coefficients:

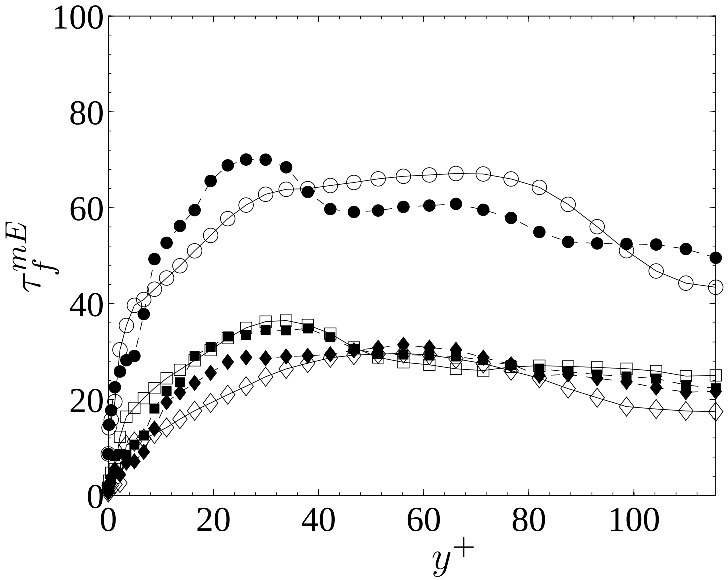

Fluid integral time scale in moving Eulerian reference frame

Filled symbols - moving with air mean velocity

open symbols - moving with particle mean velocity

stream wise $\circ$, span wise $\square$,

wall normal $\diamond$.

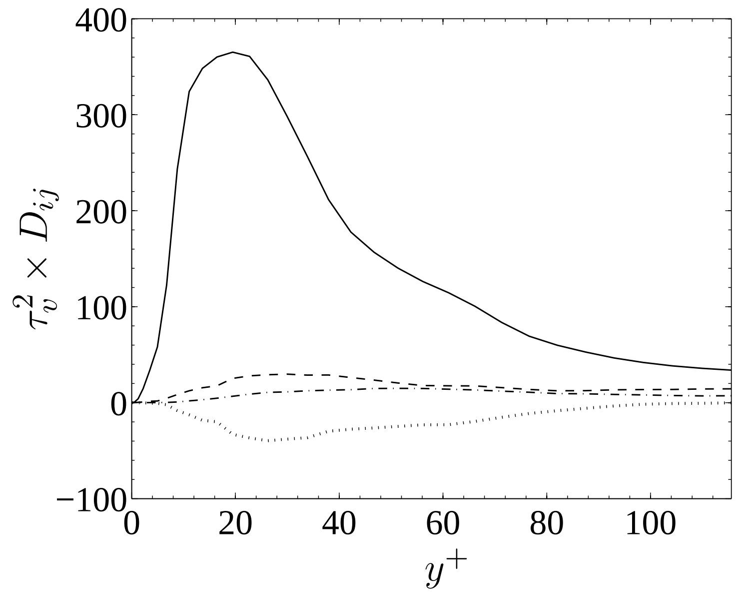

Velocity space diffusion coefficient across the width of the channel

D_{xx} (—), D_{yy} $(-.-)$, D_{zz} $(--)$, D_{xy} $(\cdots)$

Results:

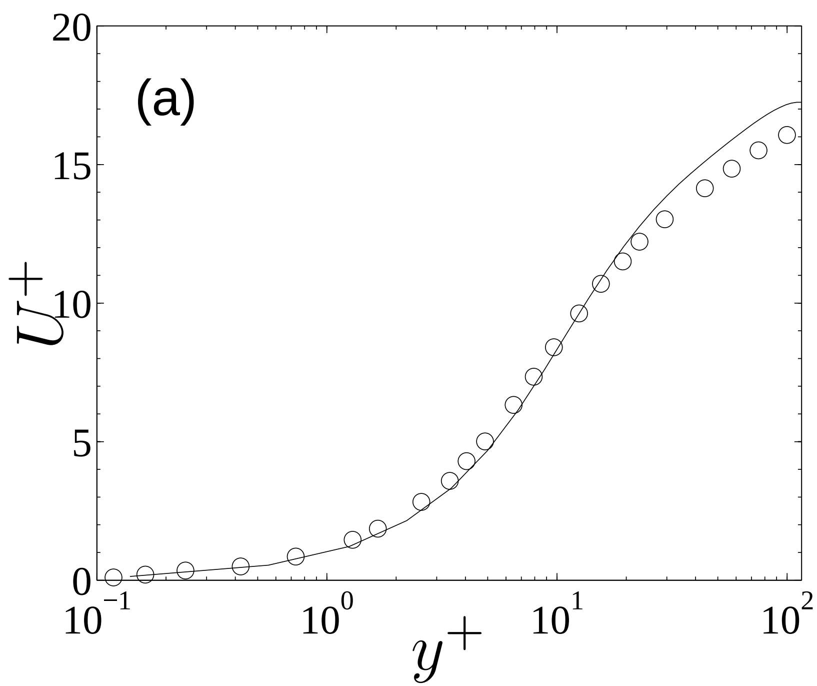

Air mean velocity; Re_c=1994

(—) is obtained from our simulation at

$Re_\tau = 115.5$,

(○) is from Mclaughlin(2001) at $Re_\tau = 125$.

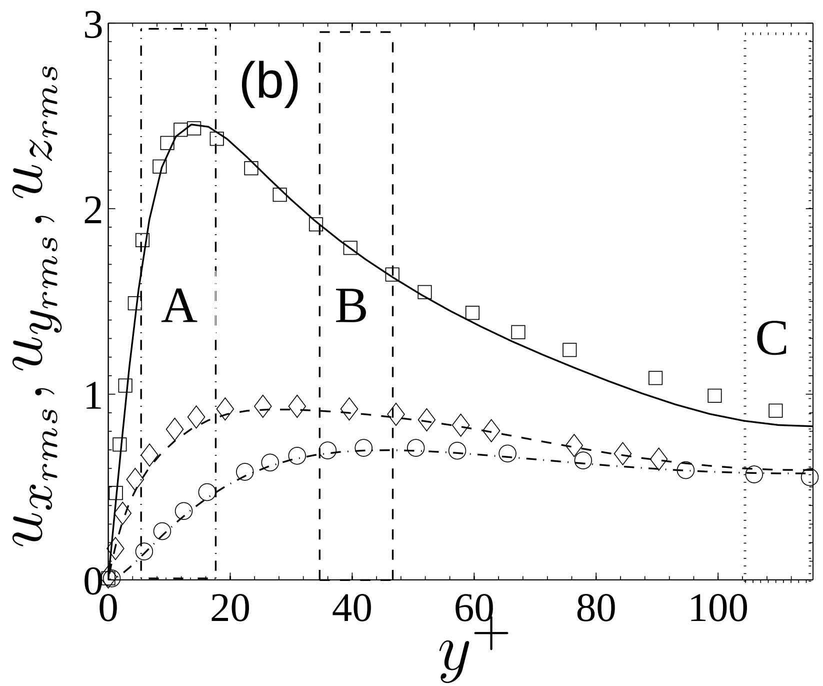

Gas-phase root-mean-square velocity fluctuation

$u_{x_{rms}}$ (—); $u_{y_{rms}}$ (-.-); $u_{z_{rms}}$ (–) are obtained from present DNS,

$u_{x_{rms}}$ (□); $u_{y_{rms}}$ (○); $u_{z_{rms}}$ (◇), obtained from Mclaughlin (2001).

Results:

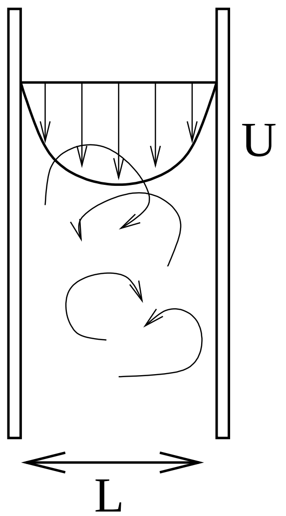

$\tau_f \sim (L/u)$

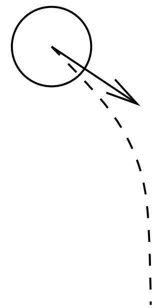

$\tau_p = (\rho_p d^2/18\eta)$

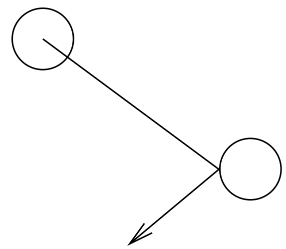

$\tau_c = (\pi \rho_s d/6 v \phi)$

- Limit $\tau_v \ll \tau_c$, $\phi = 9.44 \times 10^{-5}$, $Re = 1994$
- Limit $\tau_c \ll \tau_v$, $\phi = 7 \times 10^{-4}$, $Re = 1994$.
- $d_p = 39 \mu$m, change mass density to change τ_v.
- $0.4 \leq (d_p/\eta_K) \leq 0.7$.

Particle acceleration distribution $\tau_v \ll \tau_c$:

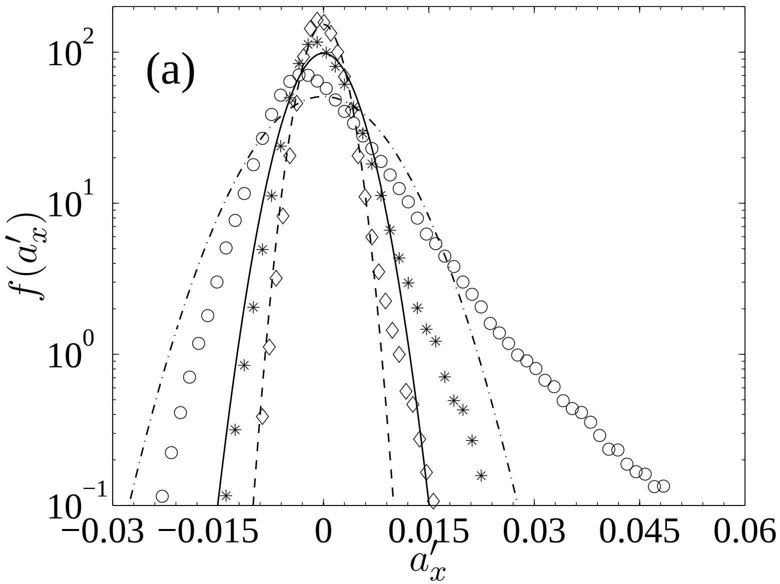

Stream wise component of acceleration distribution function at the center of the channel.

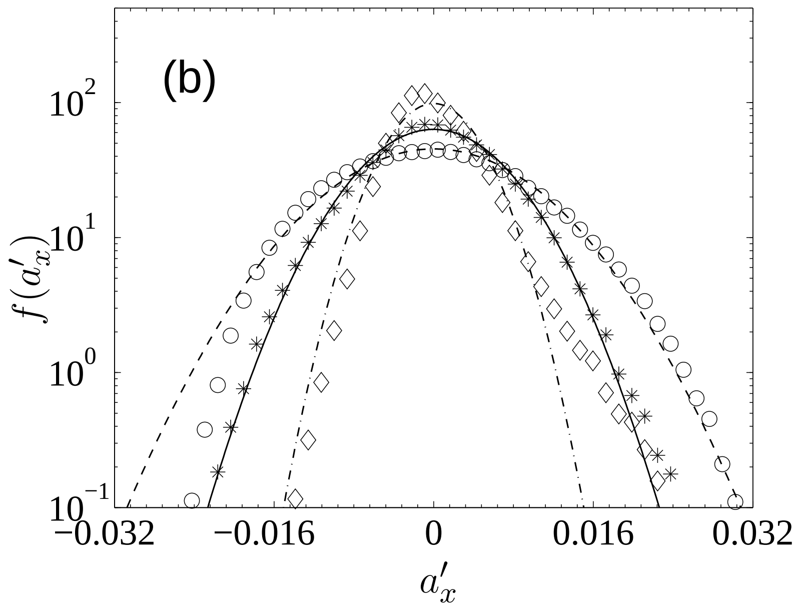

Stream wise component of particle acceleration distribution function at different cross-stream positions of the channel.

A ($\circ$); B ($*$); C ($\diamond$).

$\tau_v = 177.7$, $\tau_{c_{pp}} = 1400.0$ ($\circ$);
$\tau_v = 355.3$, $\tau_{c_{pp}} = 1650.3$ ($*$);
$\tau_v = 533.0$, $\tau_{c_{pp}} = 1807.7$ ($\diamond$).

Particle acceleration distribution $\tau_v < \tau_c$

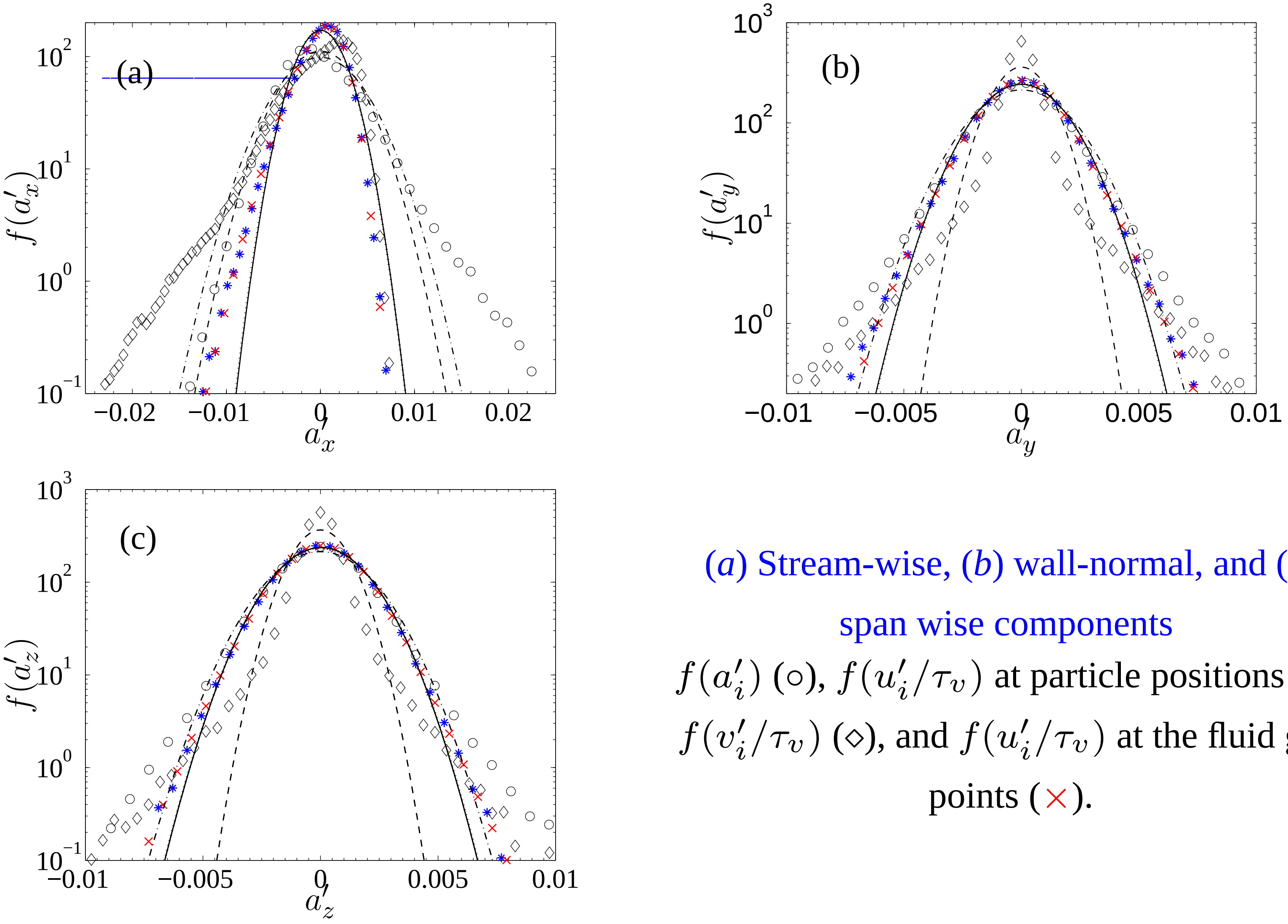

(a) Stream-wise, (b) wall-normal, and (c) span wise components

$f(a_i')$ ($\circ$), $f(u_i'/\tau_v)$ at particle positions ($*$), $f(v_i'/\tau_v)$ ($\diamond$), and $f(u_i'/\tau_v)$ at the fluid grid points ($\times$).

Particle velocity and concentration, $(\tau_v < \tau_c)$

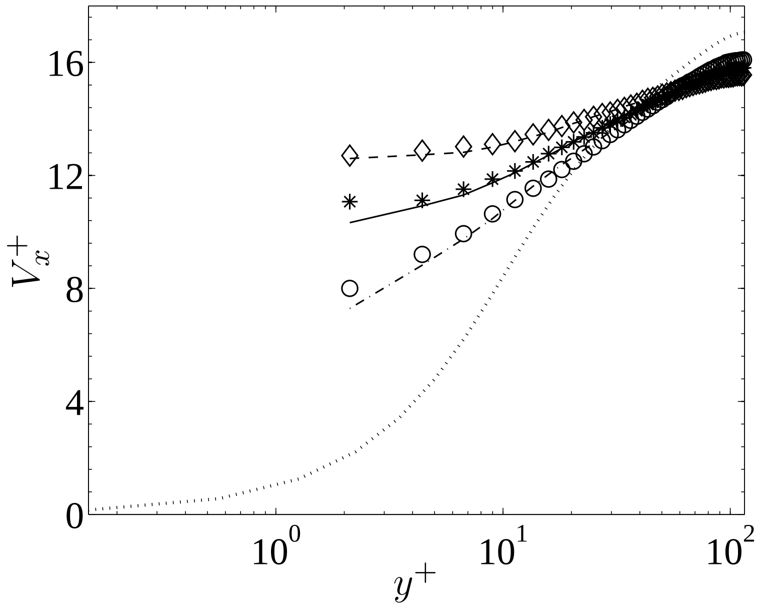

Stream-wise mean velocity of the particle phase

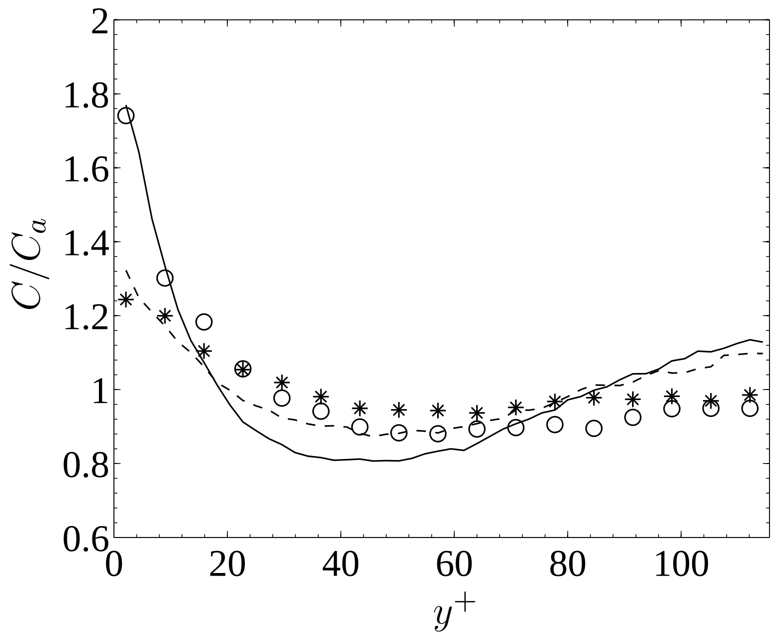

Normalized particle concentration

$\tau_v = 177.7$, $\tau_{c_{pp}} = 1400.0$, $\tau_{c_{pw}} = 925.9$, DNS ($\circ$), FFS ($-.-$);

$\tau_v = 355.3$, $\tau_{c_{pp}} = 1650.3$, $\tau_{c_{pw}} = 990.1$, DNS ($*$), FFS (—);

$\tau_v = 710.6$, $\tau_{c_{pp}} = 1999.0$, $\tau_{c_{pw}} = 1016.4$, DNS ($\diamond$), FFS ($--$)

Air velocity profile ($\cdots$).

Particle velocity fluctuation ($\tau_v < \tau_c$)

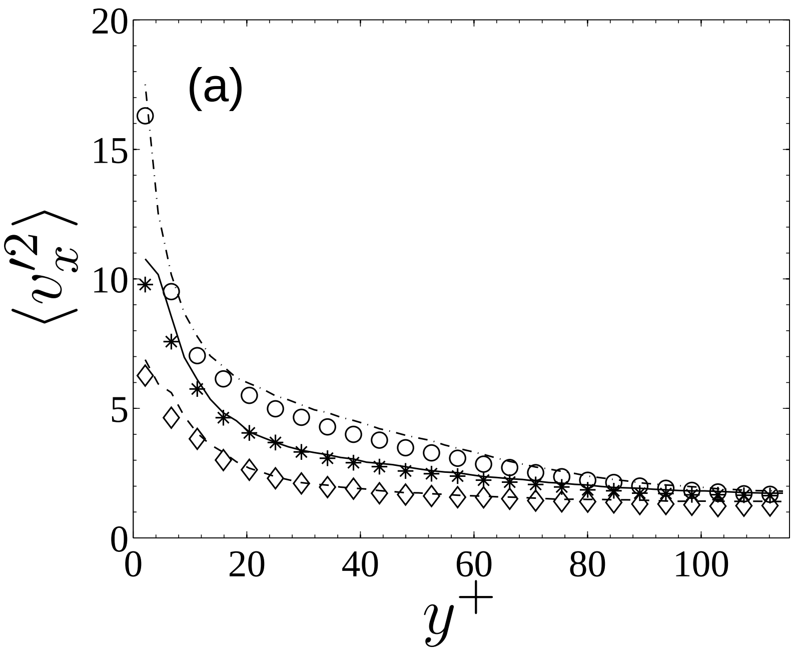

Variation of the second moment $\langle v_x'^2 \rangle$ of the particle velocity distribution

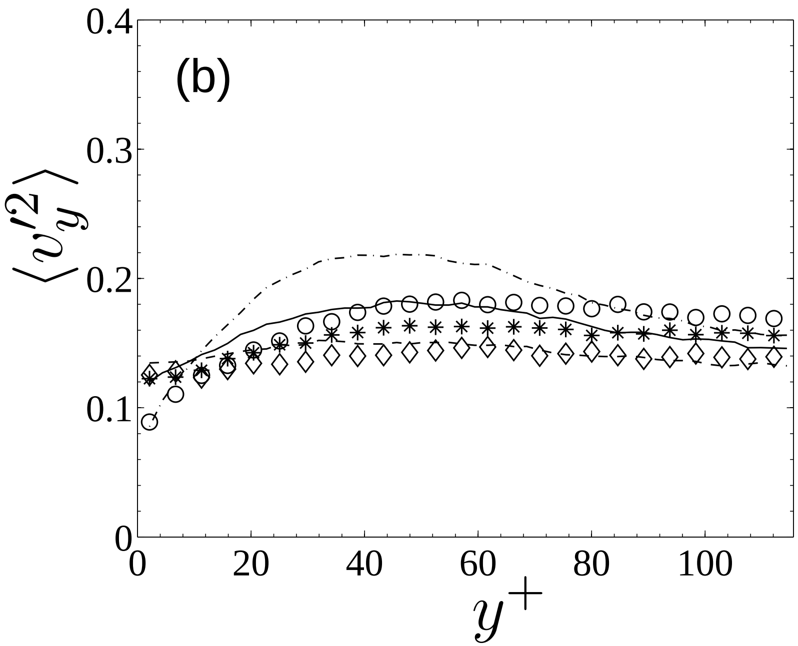

Variation of the second moment $\langle v_y'^2 \rangle$ of the particle velocity distribution

$\tau_v = 177.7$, $\tau_{c_{pp}} = 1400.0$, $\tau_{c_{pw}} = 925.9$, DNS ($\circ$), FFS (–.–);
$\tau_v = 355.3$, $\tau_{c_{pp}} = 1650.3$, $\tau_{c_{pw}} = 990.1$, DNS ($*$), FFS (—);
$\tau_v = 710.6$, $\tau_{c_{pp}} = 1999.0$, $\tau_{c_{pw}} = 1016.4$, DNS ($\diamond$), FFS (– –)
Air velocity profile ($\cdots$).

Particle velocity fluctuation ($\tau_v < \tau_c$)

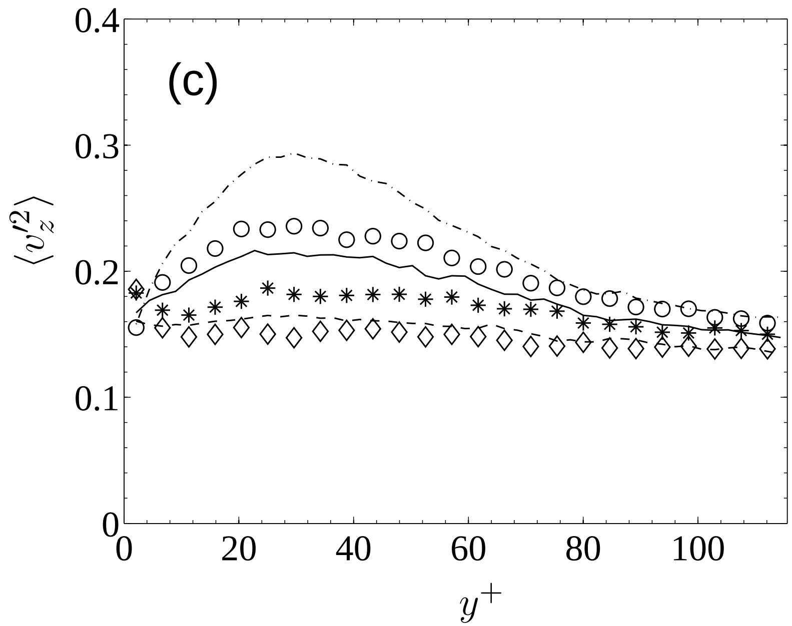

Variation of the second moment $\langle v_z'^2 \rangle$ of the particle velocity distribution

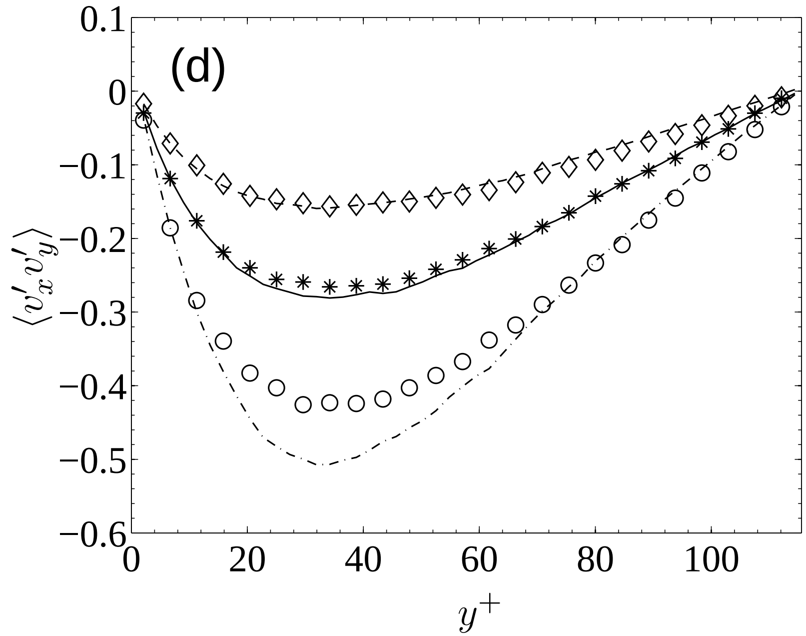

Variation of the second moment $\langle v_x' v_y' \rangle$ of the particle velocity distribution

$\tau_v = 177.7$, $\tau_{c_{pp}} = 1400.0$, $\tau_{c_{pw}} = 925.9$, DNS ($\circ$), FFS (—.—);
$\tau_v = 355.3$, $\tau_{c_{pp}} = 1650.3$, $\tau_{c_{pw}} = 990.1$, DNS ($*$), FFS (—);
$\tau_v = 710.6$, $\tau_{c_{pp}} = 1999.0$, $\tau_{c_{pw}} = 1016.4$, DNS ($\diamond$), FFS (− −)
Air velocity profile ($\cdots$).

Particle velocity distribution ($\tau_v < \tau_c$)

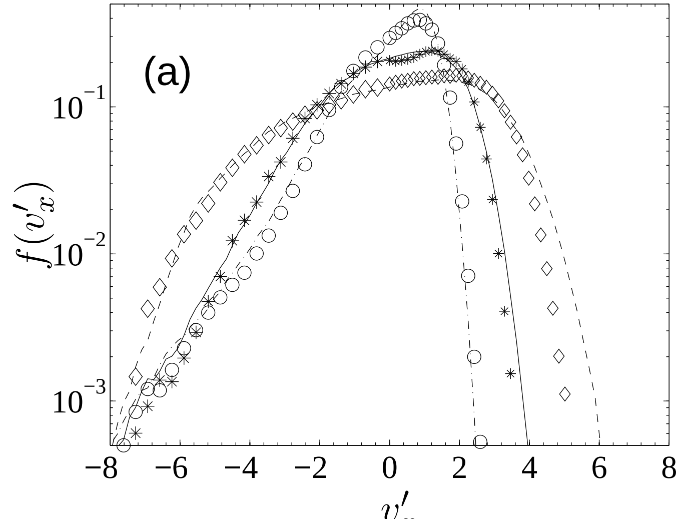

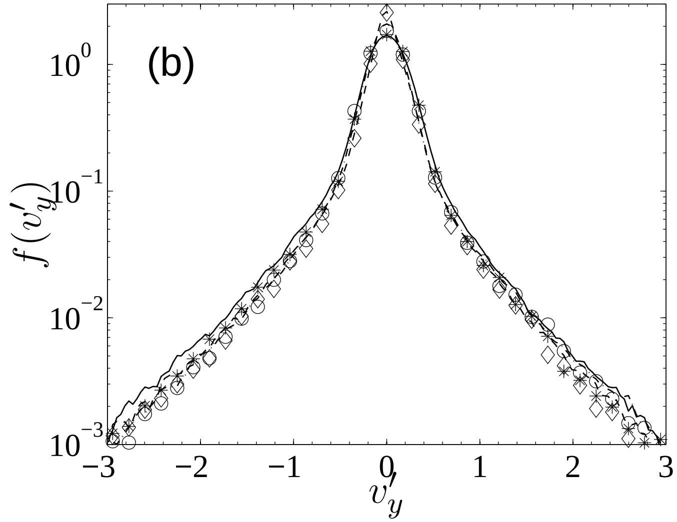

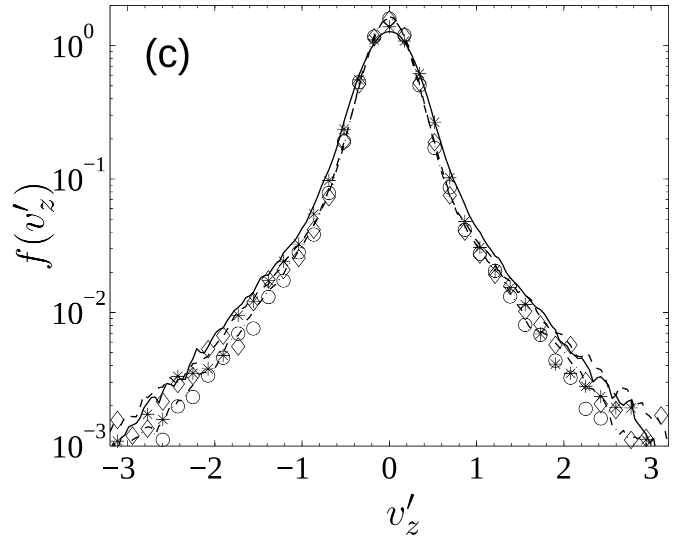

(a) Stream-wise, (b) wall-normal, and (c) span wise components

at positions A, DNS ($\diamond$), FFS ($--$);

B, DNS ($*$), FFS (—);

C, DNS ($\circ$), FFS ($-.-$).

Particle velocity and concentration, $(\tau_c < \tau_v)$

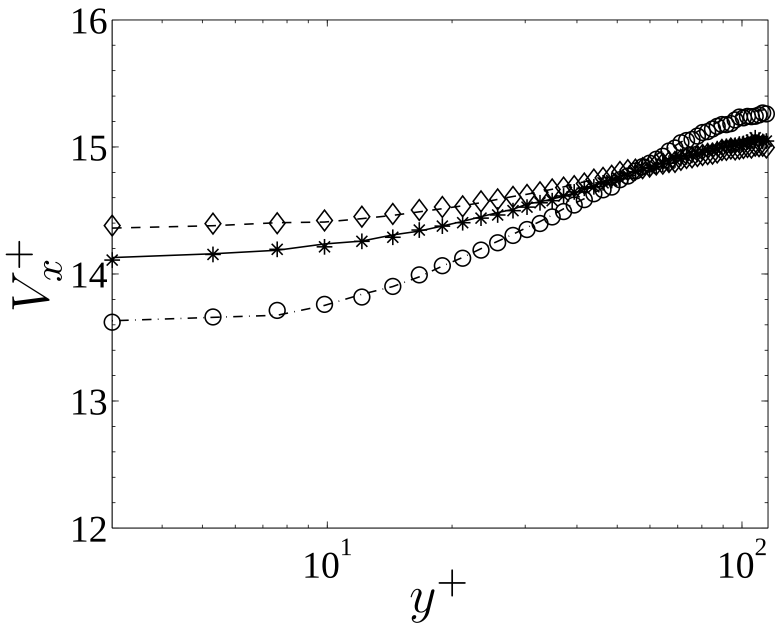

Stream-wise mean velocity of the particle phase

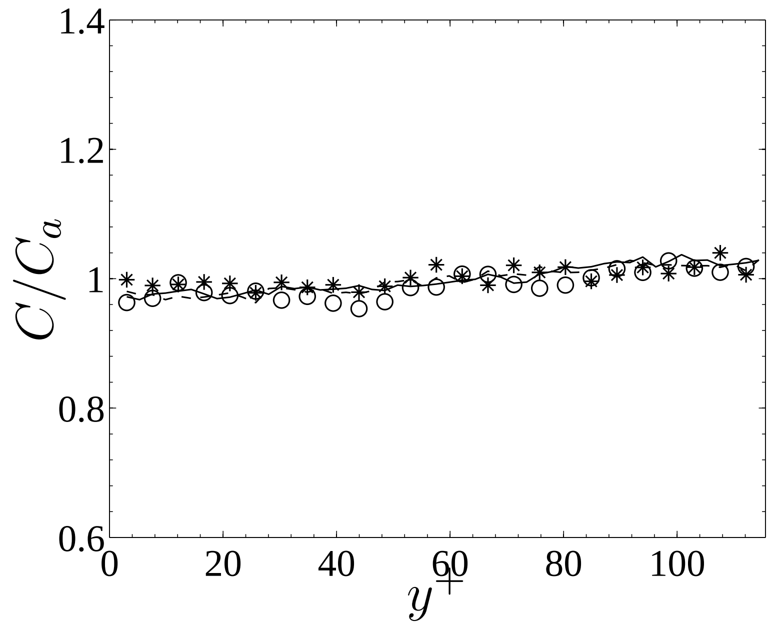

Normalized particle concentration

$\tau_v = 675.6$, $\tau_{c_{pp}} = 617.4$, $\tau_{c_{pw}} = 777.6$, DNS ($\circ$), FFS (—.—) ;
$\tau_v = 1351.1$, $\tau_{c_{pp}} = 774.3$, $\tau_{c_{pw}} = 846.2$, DNS ($*$), FFS (—);
$\tau_v = 2026.6$, $\tau_{c_{pp}} = 912.0$, $\tau_{c_{pw}} = 939.6$, DNS ($\diamond$), FFS (– –) ;

Particle velocity fluctuation ($\tau_c < \tau_v$)

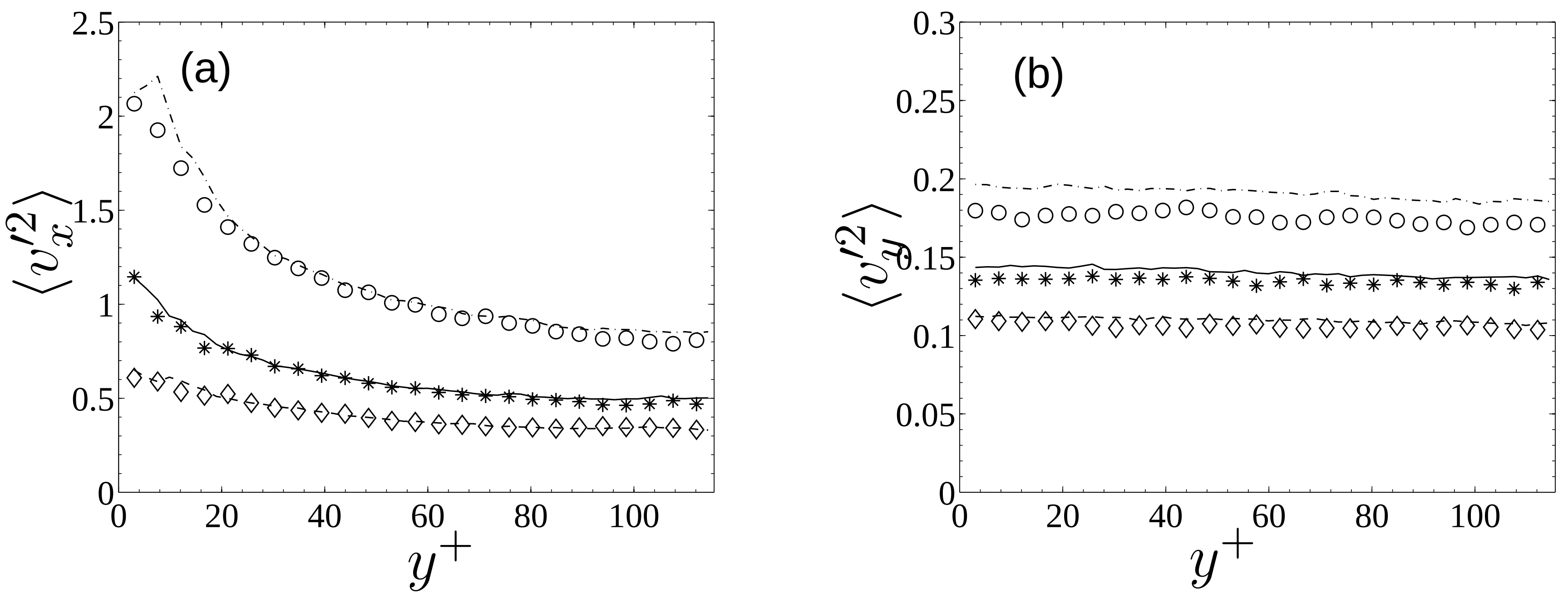

Variation of the second moment $\langle v_x'^2 \rangle$ of the particle velocity distribution

Variation of the second moment $\langle v_y'^2 \rangle$ of the particle velocity distribution

$\tau_v = 675.6$, $\tau_{c_{pp}} = 617.4$, $\tau_{c_{pw}} = 777.6$, DNS ($\circ$);
$\tau_v = 1351.1$, $\tau_{c_{pp}} = 774.3$, $\tau_{c_{pw}} = 846.2$, DNS ($*$);
$\tau_v = 2026.6$, $\tau_{c_{pp}} = 912.0$, $\tau_{c_{pw}} = 939.6$, DNS ($\diamond$)

Particle velocity fluctuation ($\tau_c < \tau_v$)

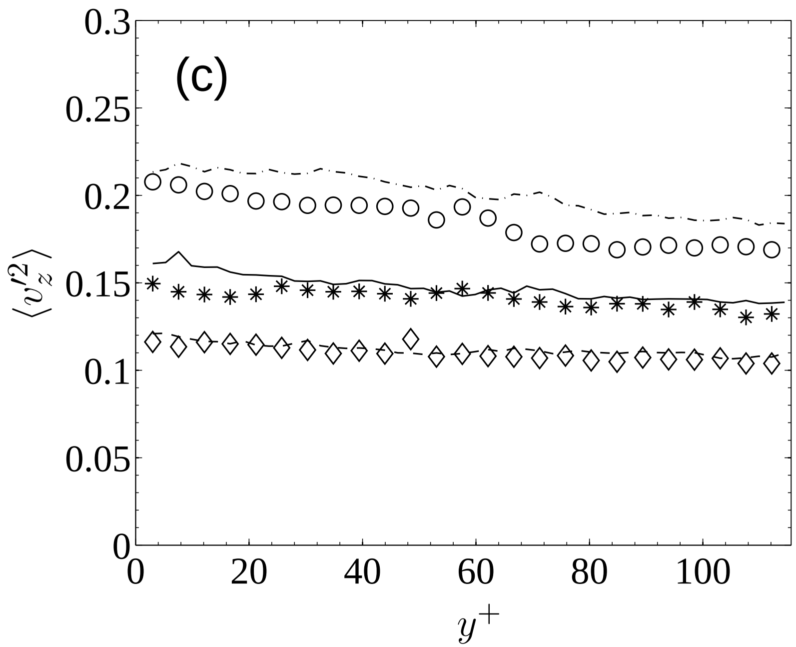

Variation of the second moment $\langle v_z'^2 \rangle$ of the particle velocity distribution

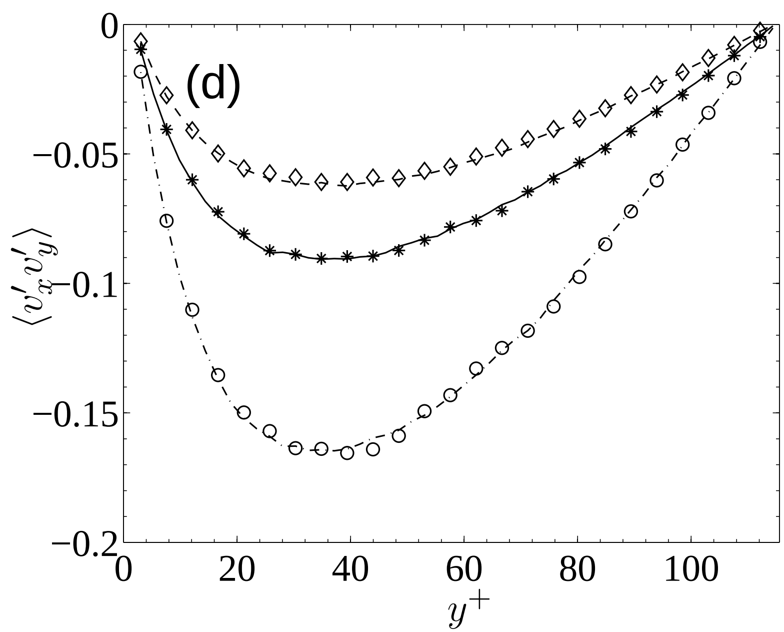

Variation of the second moment $\langle v_x' v_y' \rangle$ of the particle velocity distribution

$\tau_v = 675.6$, $\tau_{c_{pp}} = 617.4$, $\tau_{c_{pw}} = 777.6$, DNS ($\circ$);

$\tau_v = 1351.1$, $\tau_{c_{pp}} = 774.3$, $\tau_{c_{pw}} = 846.2$, DNS ($*$);

$\tau_v = 2026.6$, $\tau_{c_{pp}} = 912.0$, $\tau_{c_{pw}} = 939.6$, DNS ($\diamond$)

Particle velocity distribution ($\tau_c < \tau_v$)

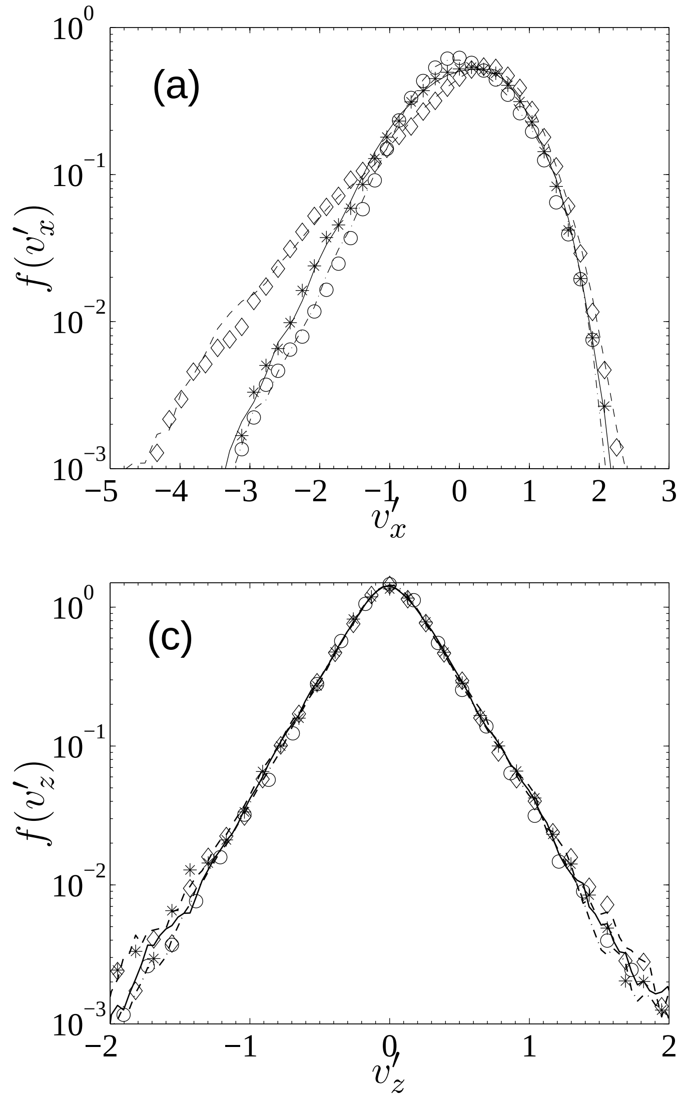

(a) Stream-wise, (b) wall-normal, and (c) span wise components

at positions A, DNS ($\diamond$), FFS (— —);

B, DNS ($*$), FFS (—);

C, DNS ($\circ$), FFS (—.—)

Particle fluctuations: Streamwise diffusion.

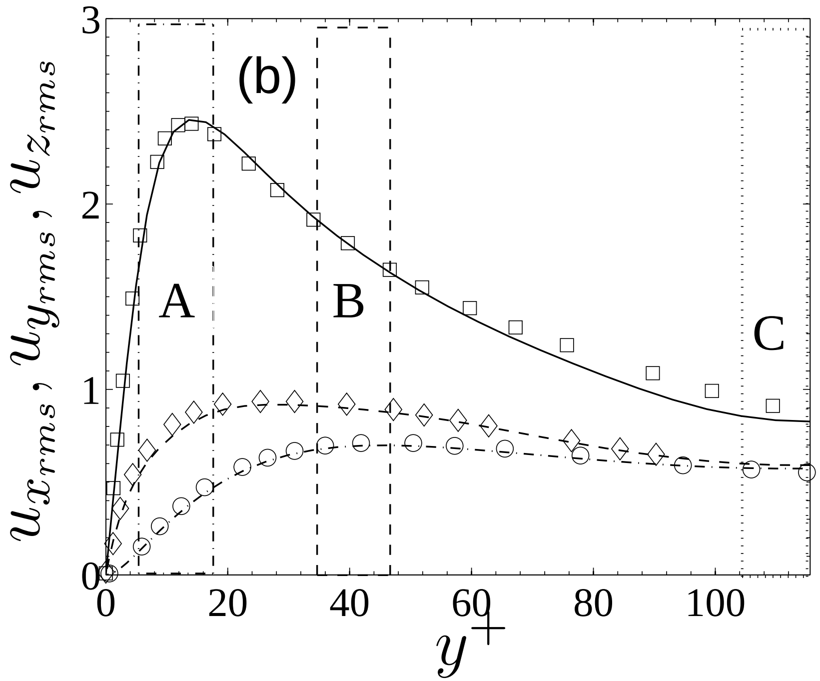

Gas-phase root-mean-square velocity fluctuation

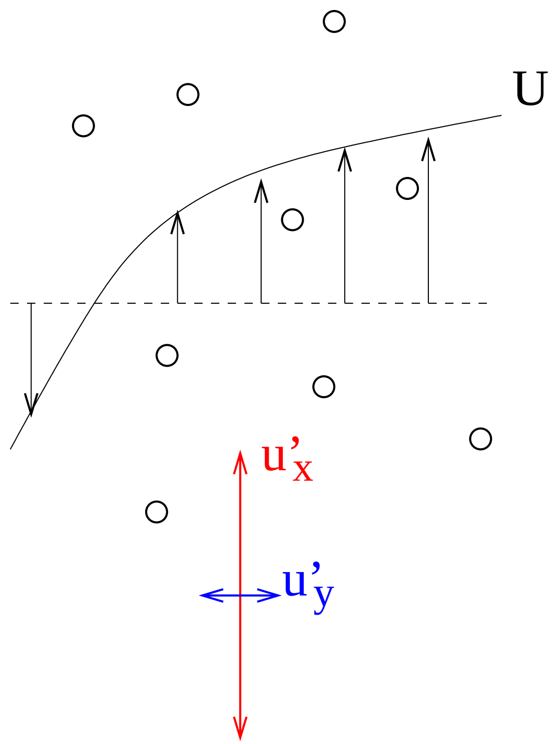

$u_{x_{rms}}$ (—); $u_{y_{rms}}$ (-.-); $u_{z_{rms}}$ (–) are obtained from present DNS,

$u_{x_{rms}}$ (□); $u_{y_{rms}}$ (○); $u_{z_{rms}}$ (◇), obtained from Mclaughlin (2001).

- $\langle v_x^2 \rangle \sim \tau_v D_{xx}$.

Particle fluctuations: Cross-stream diffusion.

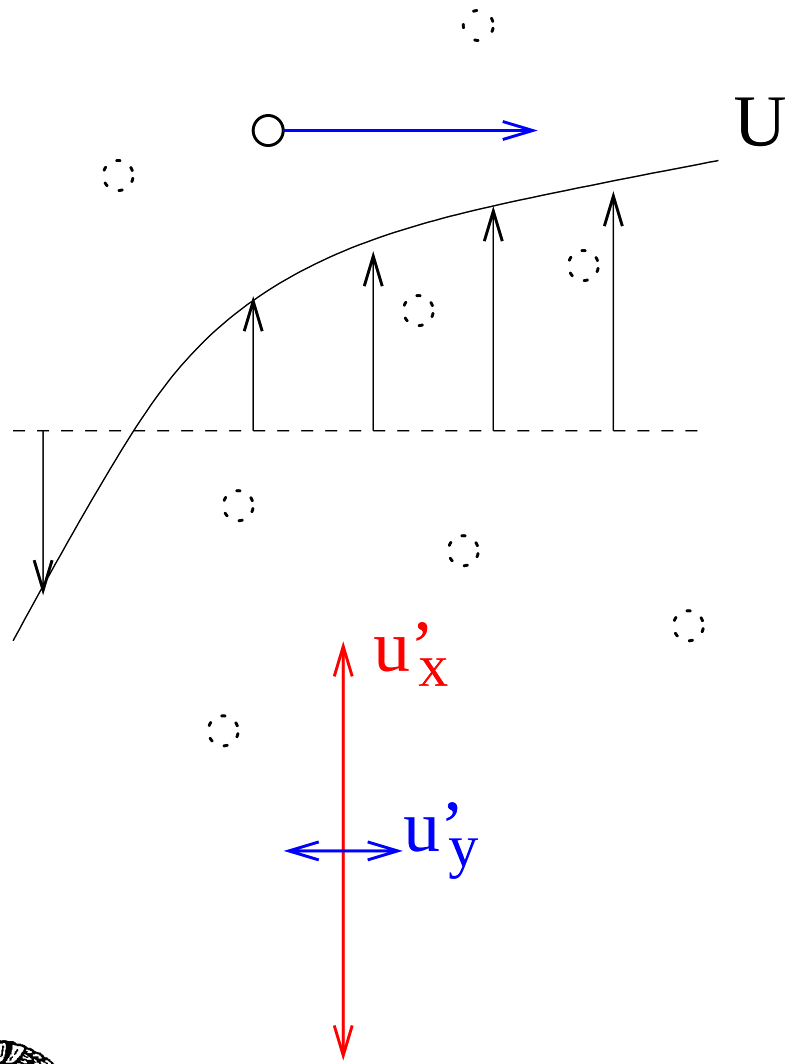

- Cross-stream fluctuations — mean square velocity $D_{yy}\tau_v$.
- Velocity fluctuation in cross-stream direction $\sqrt{D_{yy}\tau_v}$.
- Distance moved $\tau_v\sqrt{D_{yy}\tau_v}$.

Particle fluctuations: Cross-stream diffusion.

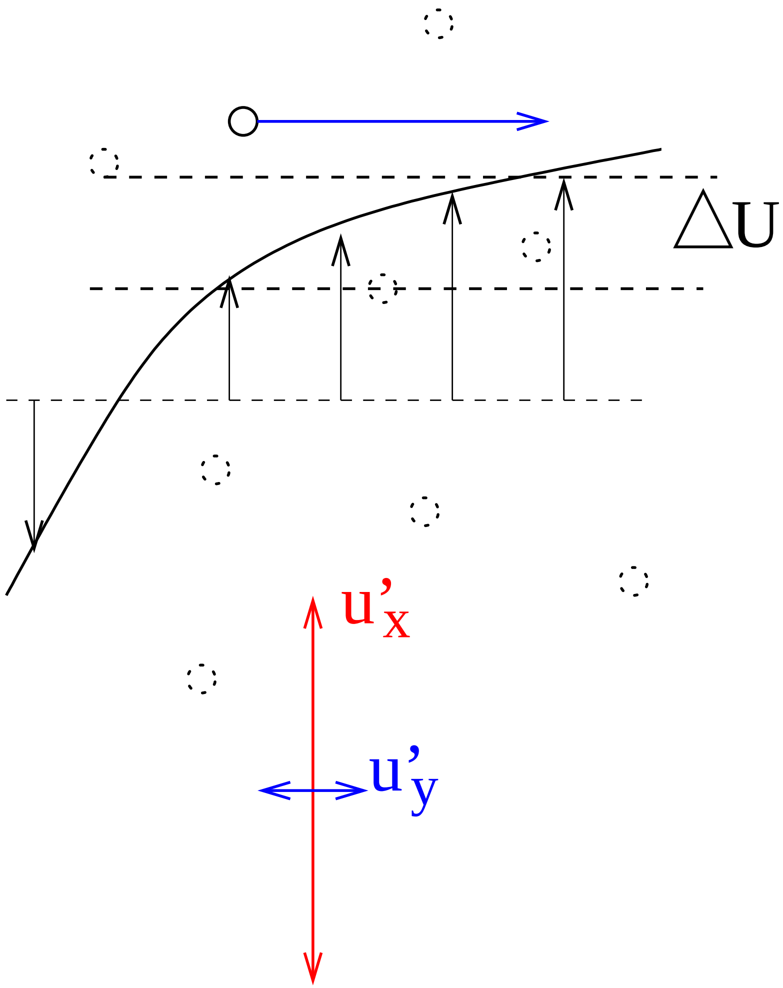

- Cross-stream fluctuations — mean square velocity $D_{yy}\tau_v$.
- Velocity fluctuation in cross-stream direction $\sqrt{D_{yy}\tau_v}$.
- Distance moved $\tau_v\sqrt{D_{yy}\tau_v}$.
- Difference in velocity $\dot{\gamma}\tau_v\sqrt{D_{yy}\tau_v}$
- Fluctuation generation $(\dot{\gamma}\tau_v)^2(D_{yy}\tau_v)$.
- $\langle v_x^2\rangle \sim \mathrm{St}_\gamma^2(D_{yy}\tau_v)$.

Particle fluctuations: Collisions due to shear.

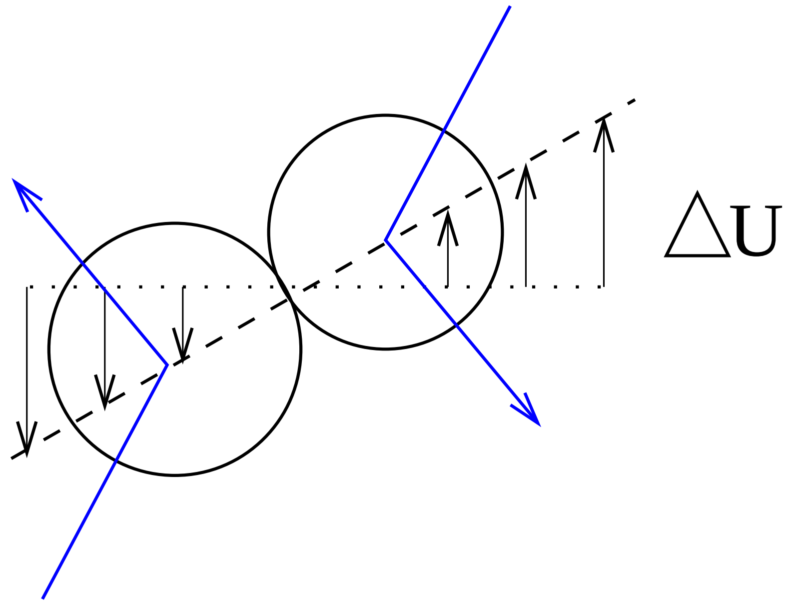

- Difference in mean velocity $\dot{\gamma} d$.
- Collision frequency $(n d^2)(\dot{\gamma} d) \sim (\phi \dot{\gamma})$.

Particle fluctuations: Collisions due to shear.

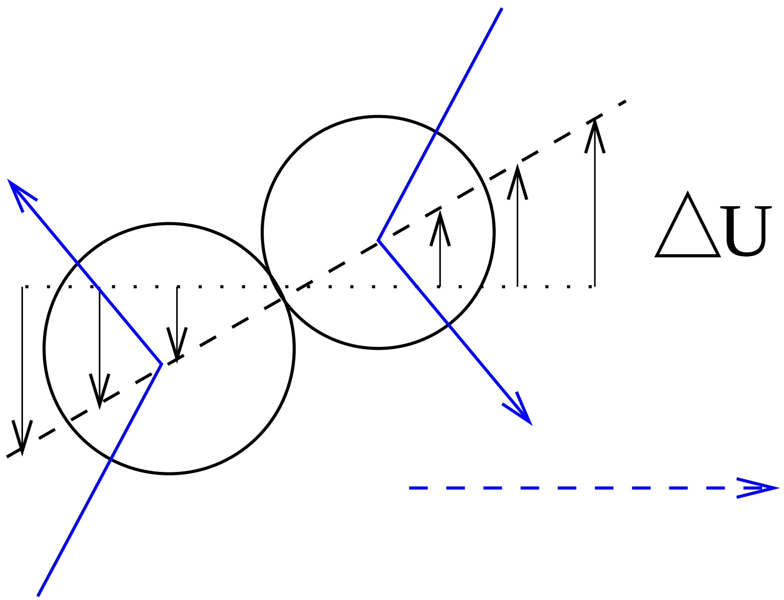

- Difference in mean velocity $\dot{\gamma} d$.
- Collision frequency $(nd^2)(\dot{\gamma} d) \sim (\phi \dot{\gamma})$.
- Distance in horizontal direction $(\dot{\gamma} d \tau_v)$; velocity difference $(\dot{\gamma} \tau_v)(\dot{\gamma} d)$.
- Streamwise fluctuating velocity generation $(\phi \dot{\gamma})(\dot{\gamma} d)^2 \mathrm{St}_\gamma^2$.
- Dissipation $(\langle v_x^2 \rangle / \tau_v)$.
- $\langle v_x^2 \rangle \sim \phi (\dot{\gamma} d)^2 \mathrm{St}_\gamma^3$

Source of particle fluctuations:

τ_v	St_γ	$(\tau_v D_{zz})$	$(\tau_v D_{yy})$	$(\tau_v D_{yy})St_\gamma^2$	$(\dot{\gamma}d)^2$	$\phi(\dot{\gamma}d)^2 St_\gamma^3$	T_{zz}
(a) At position A ($y^+ = 5.8$ - 17.3)							
177.66	44.31	2.0	0.026	51.57	0.234	1.927	8.05
355.32	54.50	1.0	0.013	39.0	0.089	1.355	6.36
532.98	63.70	0.67	0.009	35.52	0.054	1.314	5.33
710.64	68.13	0.50	0.007	30.48	0.035	1.035	4.25
(b) At position B ($y^+ = 34.7$ - 46.2)							
177.66	10.08	1.10	0.074	7.57	0.012	1.17×10^{-3}	4.38
355.32	15.30	0.55	0.037	8.73	0.007	2.37×10^{-3}	2.96
532.98	17.75	0.36	0.025	7.57	0.004	2.21×10^{-3}	2.32
710.64	23.66	0.27	0.019	10.43	0.002	2.96×10^{-3}	1.88
(c) At position C ($y^+ = 104.0$ - 115.5)							
177.66	1.056	0.196	0.040	0.045	1.33×10^{-4}	1.48×10^{-8}	1.83
355.32	1.331	0.098	0.020	0.035	5.29×10^{-5}	1.18×10^{-8}	1.74
532.98	1.535	0.065	0.013	0.031	3.13×10^{-5}	1.07×10^{-8}	1.57
710.64	1.597	0.049	0.010	0.025	1.90×10^{-5}	7.32×10^{-9}	1.41

Particle fluctuations: Cross-stream

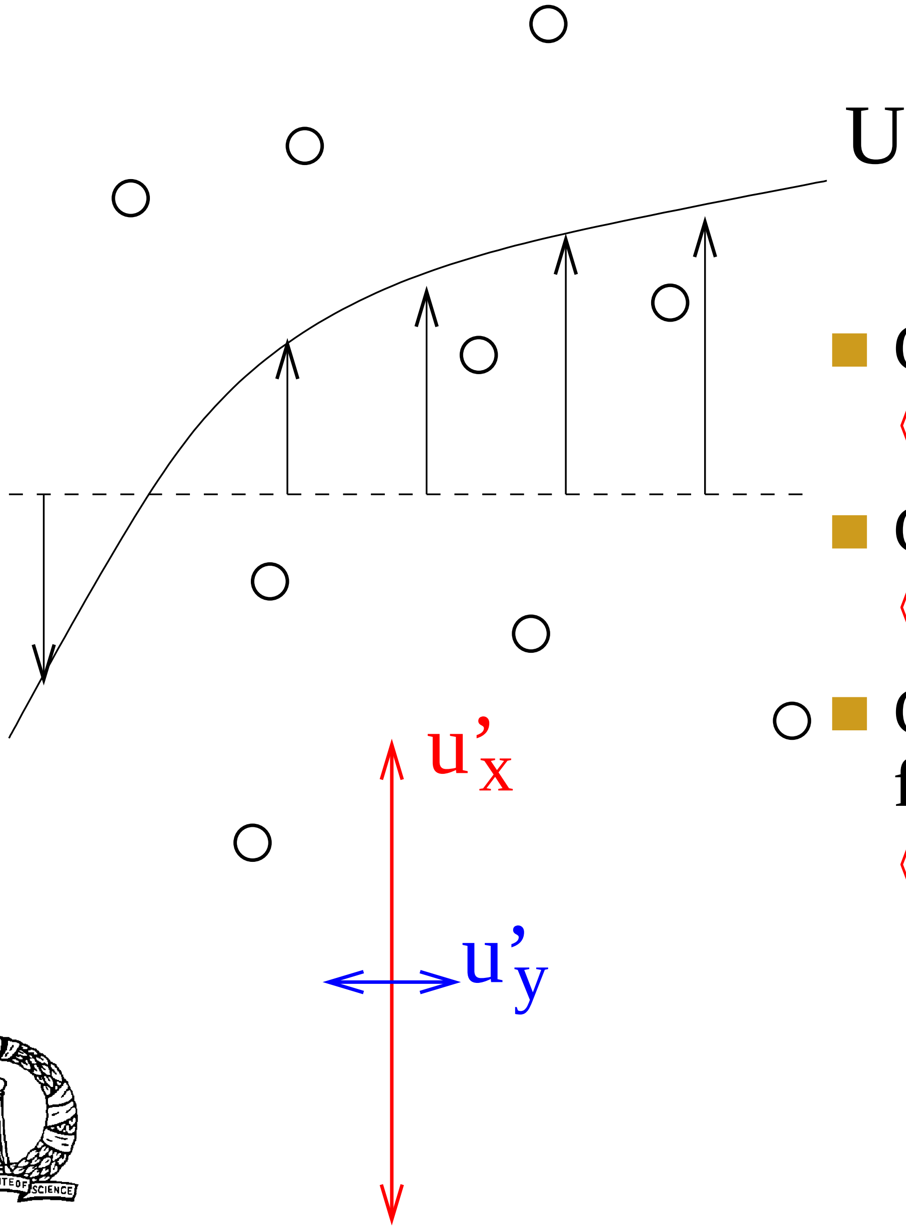

- Cross-stream diffusion:
  $\langle v_y^2 \rangle \sim D_{yy} \tau_v$
- Collisions due to shear:
  $\langle v_y^2 \rangle \sim \phi (\dot{\gamma} d)^2 \mathrm{St}_\gamma$
- Collisions due to streamwise fluctuations:
  $\langle v_y^2 \rangle \sim \phi (\langle v_x^2 \rangle)^{3/2} (\tau_v / d)$

Source of particle fluctuations:

τ_v	St_γ	$(\tau_v D_{yy})$	$(\dot{\gamma} d)^2$	$\phi(\dot{\gamma} d)^2 St_\gamma$	T_{xx}	$\phi(T_{xx}^{1/2}\tau_v/d)T_{xx}$	T_{yy}
(*a*) At position A ($y^+ = 5.8$ - 17.3)							
177.7	44.31	0.026	0.235	9.81×10^{-4}	8.05	0.197	0.159
355.3	54.5	0.013	0.089	4.57×10^{-4}	6.36	0.277	0.153
533.0	63.7	0.009	0.054	3.24×10^{-4}	5.33	0.319	0.152
710.6	54.82	0.007	0.022	1.16×10^{-4}	4.25	0.303	0.150
(*b*) At position B ($y^+ = 34.7$ - 46.2)							
177.7	10.08	0.074	0.012	1.15×10^{-5}	4.38	0.079	0.242
355.3	15.30	0.037	0.007	1.01×10^{-5}	2.96	0.088	0.195
533.0	17.75	0.025	0.004	7.0×10^{-6}	2.32	0.091	0.180
710.6	23.66	0.019	0.002	5.29×10^{-6}	1.88	0.089	0.163
(*c*) At position C ($y^+ = 104.0$ - 115.5)							
177.7	1.056	1.33×10^{-4}	6.25×10^{-5}	1.33×10^{-8}	1.83	0.021	0.175
355.3	1.331	5.29×10^{-5}	1.73×10^{-4}	6.64×10^{-9}	1.74	0.020	0.160
533.0	1.535	3.13×10^{-5}	$3.13 \times 10 - 5$	4.53×10^{-9}	1.57	0.017	0.156
710.6	1.597	1.90×10^{-5}	1.36×10^{-5}	2.87×10^{-9}	1.41	0.014	0.145

Summary

- Distributions are highly non-Gaussian near the center of the channel, event though fluctuating force is Gaussian.
- Distributions are closer to a Gaussian at the locations away from the channel center, especially in regions where the variances of the fluid velocity fluctuations are a maximum.
- Time correlation of the particle acceleration fluctuations is close to the time correlations of the fluid velocity in a ‘moving Eulerian’ reference moving with the mean fluid velocity.
- Quantitative agreement between distributions from DNS and fluctuating force simulations with one-way coupling.
- Source of fluctuations complicated — involves streamwise and cross-stream diffusion and collisions.

INDIAN INSTITUTE OF SCIENCE

Experiments on particle laden Channel flow

Experimental setup

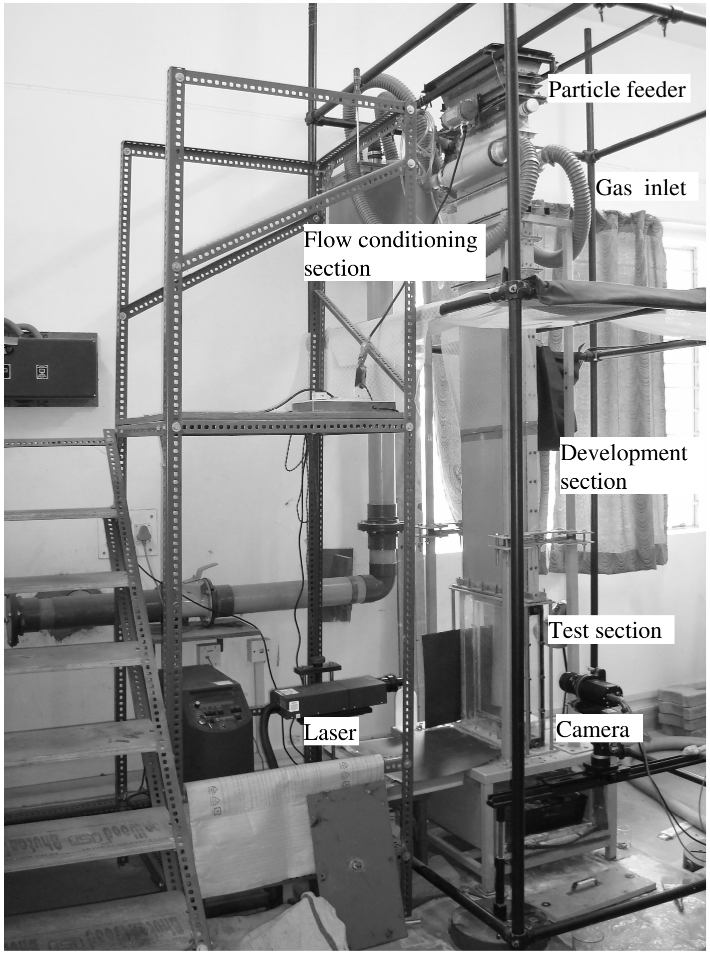

Photograph of setup

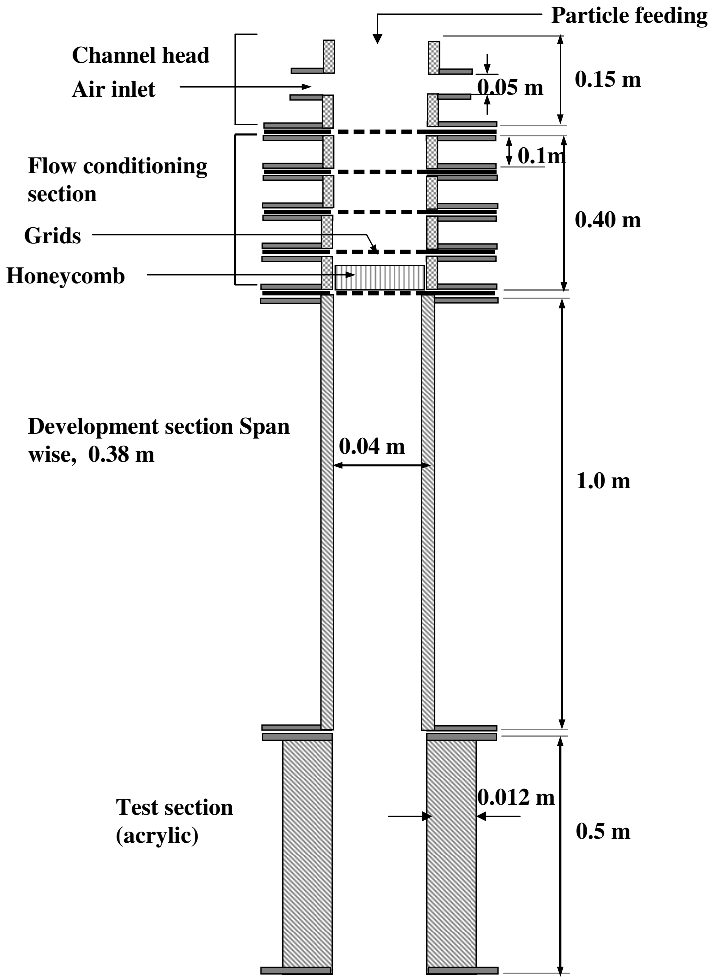

Sectional view

Experimental setup

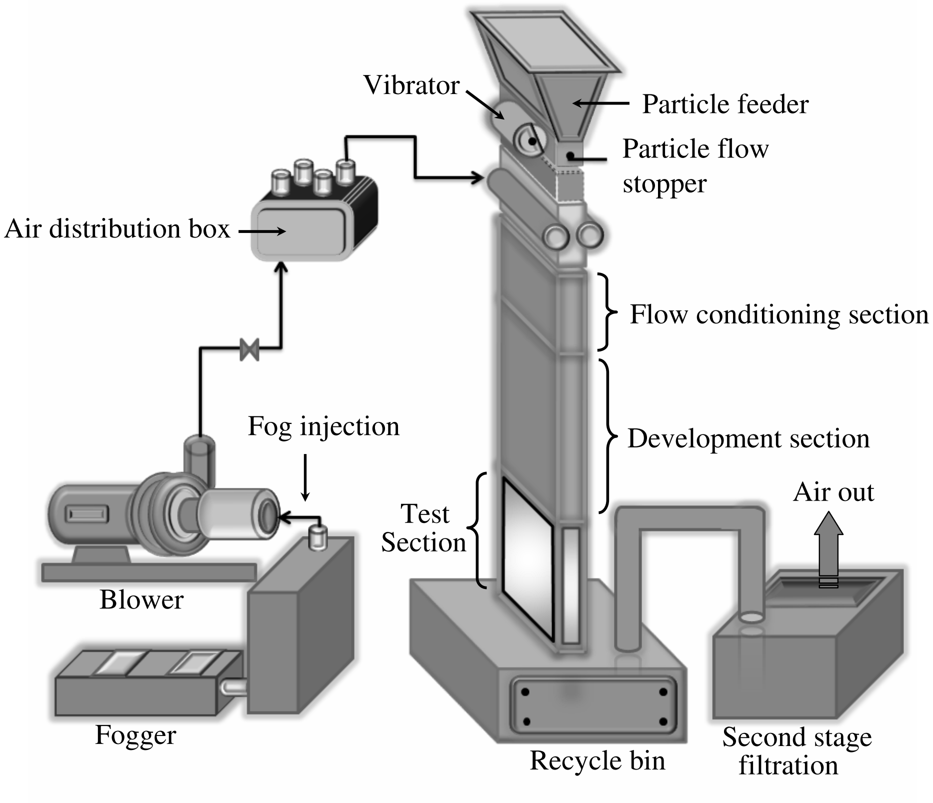

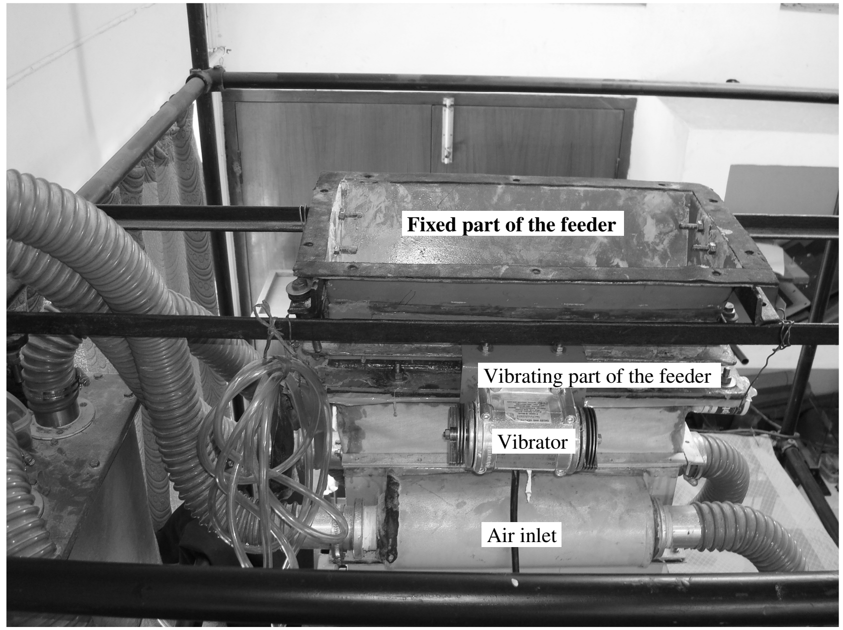

Components of PIV

- CCD Camera
- Nd:YAG pulsed Laser
- Timing control module for synchronization of the laser and camera
- Seeding arrangements
- Image processing software
- Laser sheet forming collimating lens

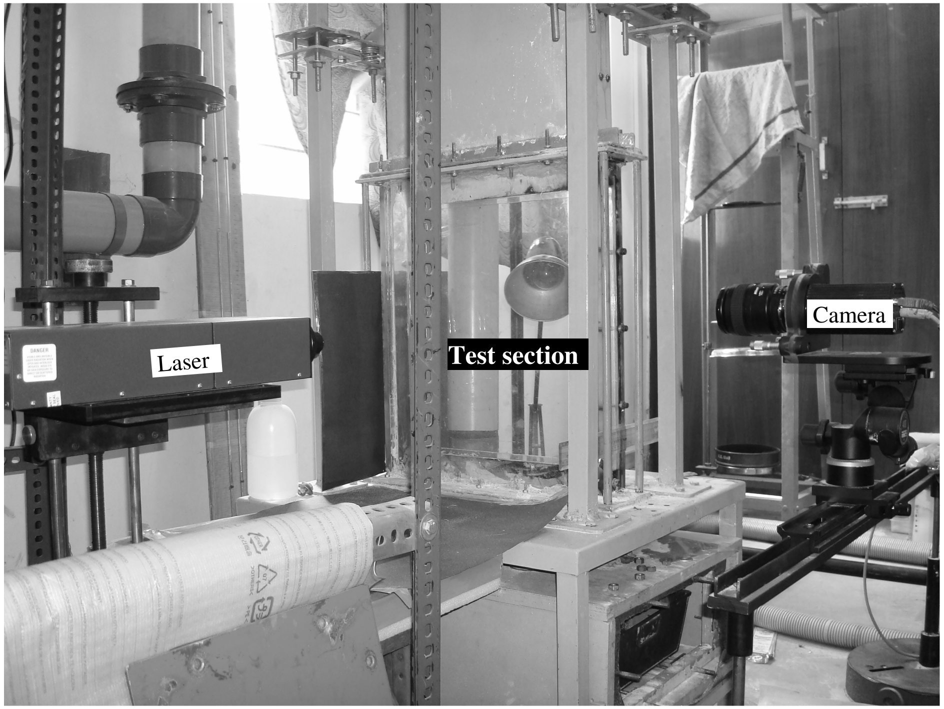

Image processing

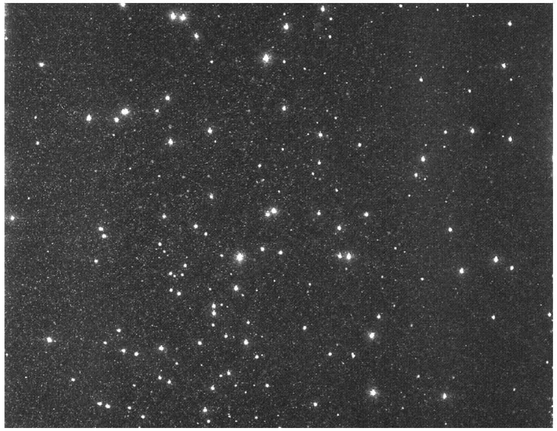

Composite image of particles and fluid tracer

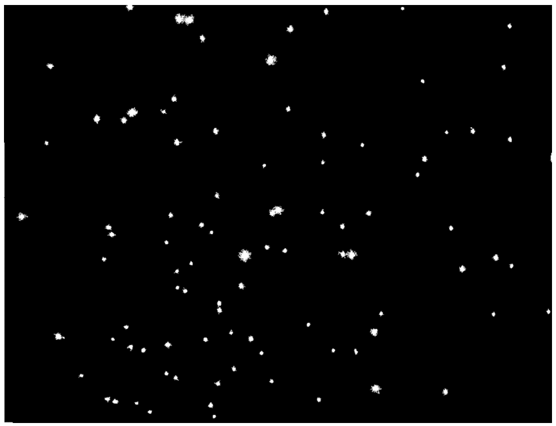

Only particles

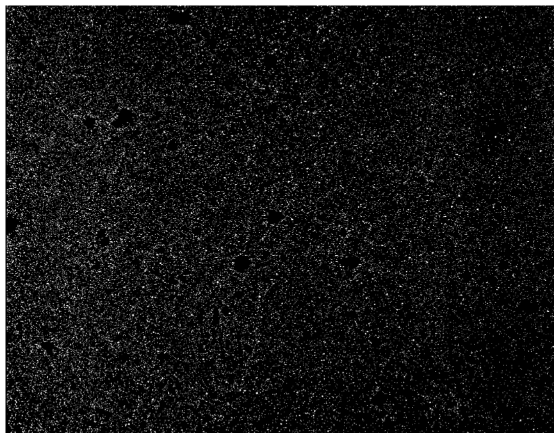

Only tracer

Validation of PIV results

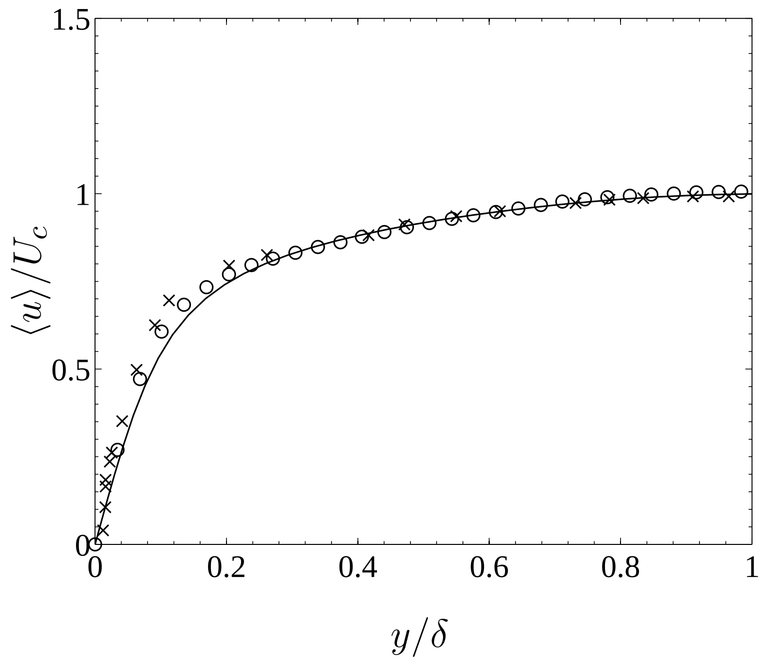

Gas-phase mean velocity profile from experiment and DNS; Re_c=20221.14.

(○) PIV, (—) DNS, × Niederschulte et al. (1990), Re_c= 3221.5.

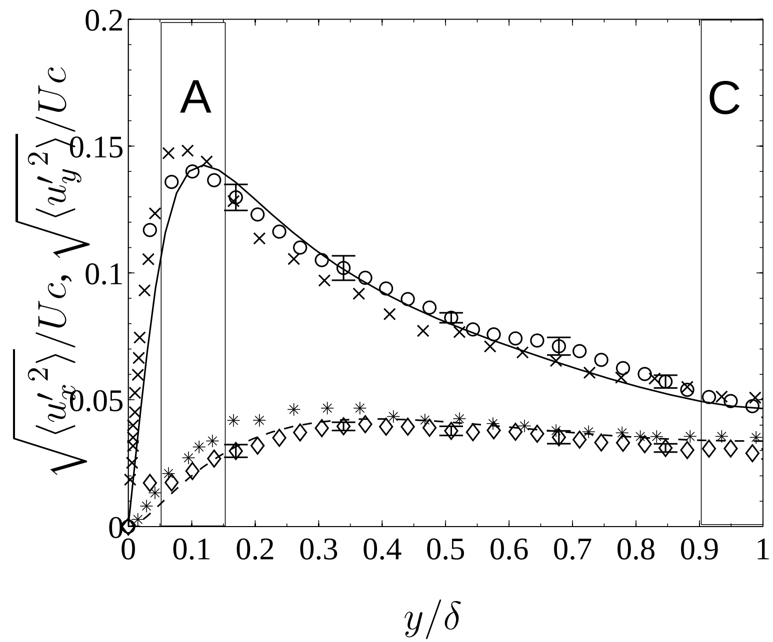

Gas-phase turbulent intensity obtained from experiment and DNS

(○) u_{rms}, PIV; (◇) v_{rms}, PIV;

(—) u_{rms}, DNS; $--$ v_{rms}, DNS; × and $*$ Niederschulte et al. (1990)

Simulations vs. Experiment: $(\tau_v < \tau_c)$ $\phi = 9 \times 10^{-5}$

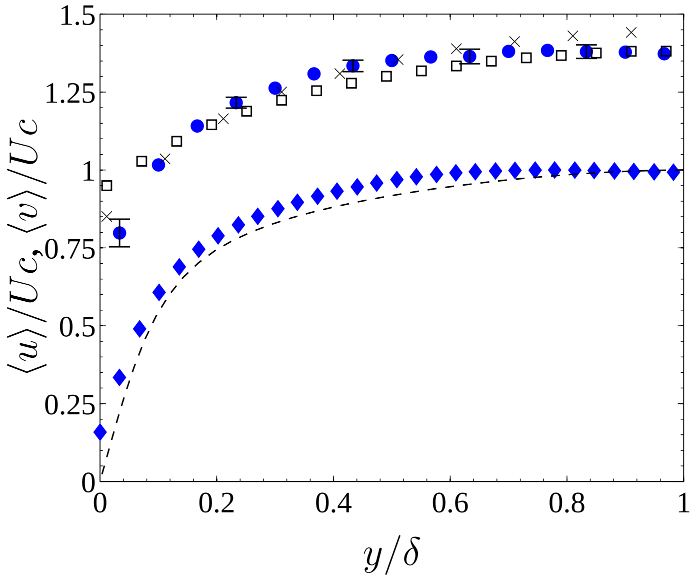

Mean stream-wise velocity of the particle.

($\bullet$), mean particle velocity (V_x); ($\blacklozenge$), mean air velocity (U_x); (——), U_x, FFS; ($\square$), V_x, $e_n = 1.0$, $e_t = 0.7$; ($\times$), V_x, $e_n = 0.7$, $e_t = 0.7$;

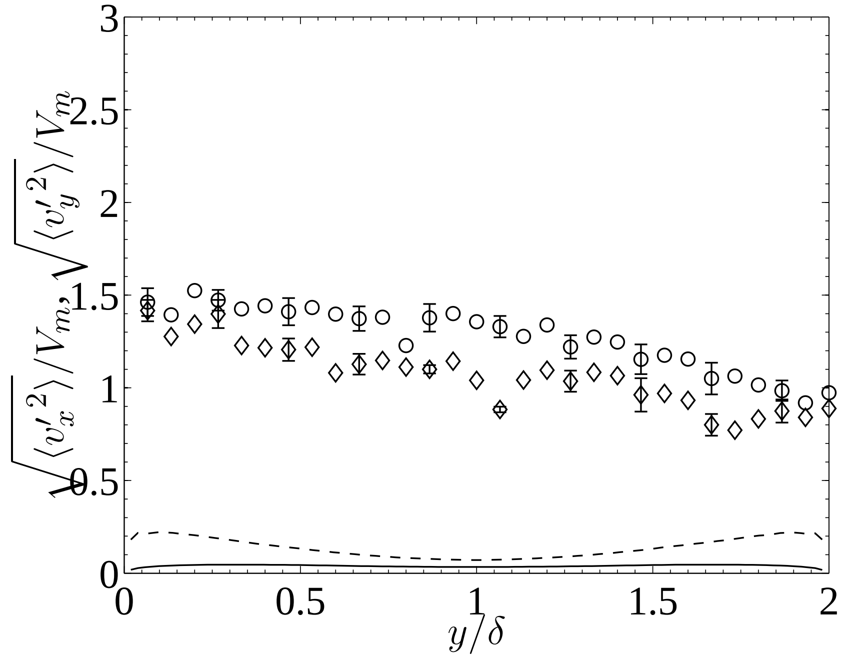

Intensity of particle phase velocity fluctuation

($\circ$) u_{rms}, Experiment; ($\diamond$) v_{rms}, Experiment; $--$ u_{rms}, FFS; (—) v_{rms}, FFS

Particle phase — polydispersity:

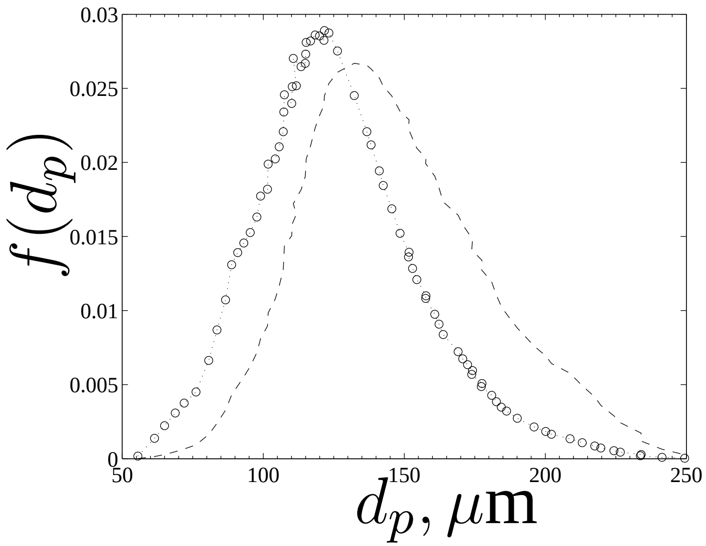

Particle size distribution, ○, number based distribution ; $--$, volume based distribution.

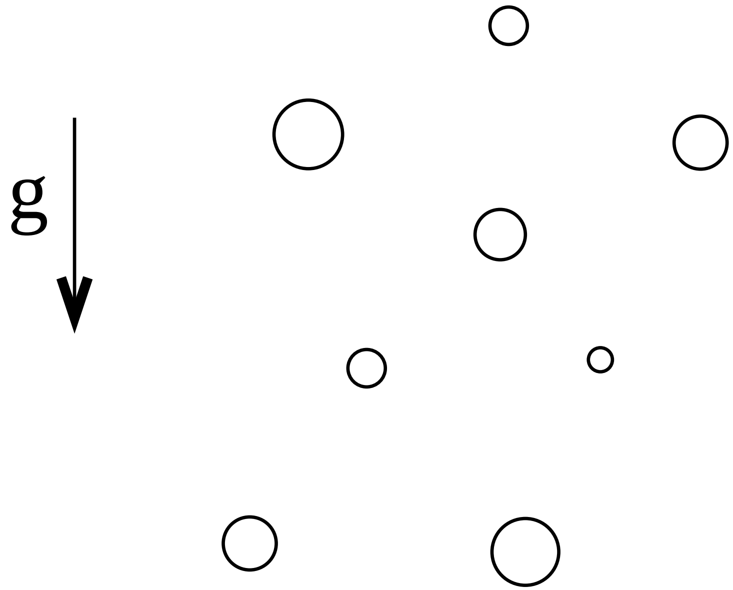

Difference in terminal velocities

...

Particle phase — polydispersity:

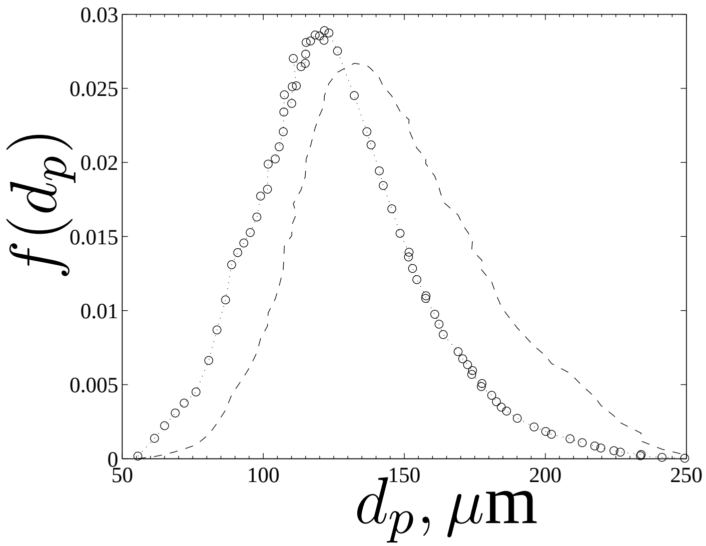

Particle size distribution, ○, number based distribution ; −−, volume based distribution.

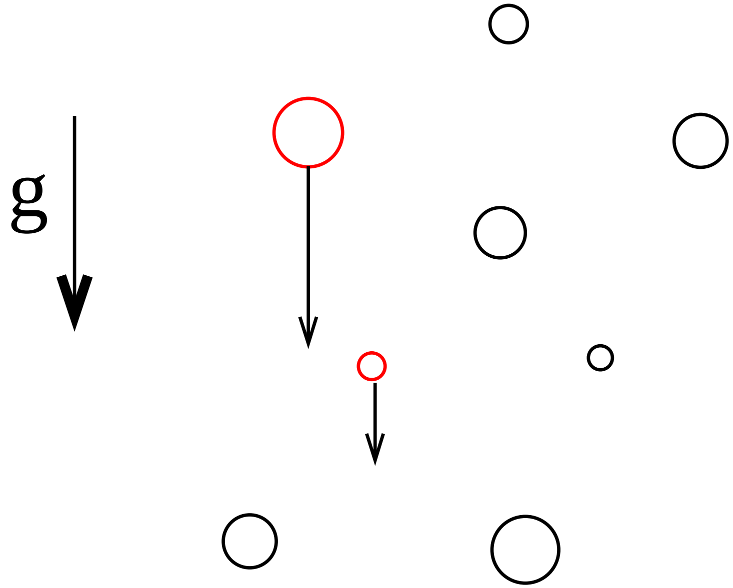

... induced collisions ...

Particle phase — polydispersity:

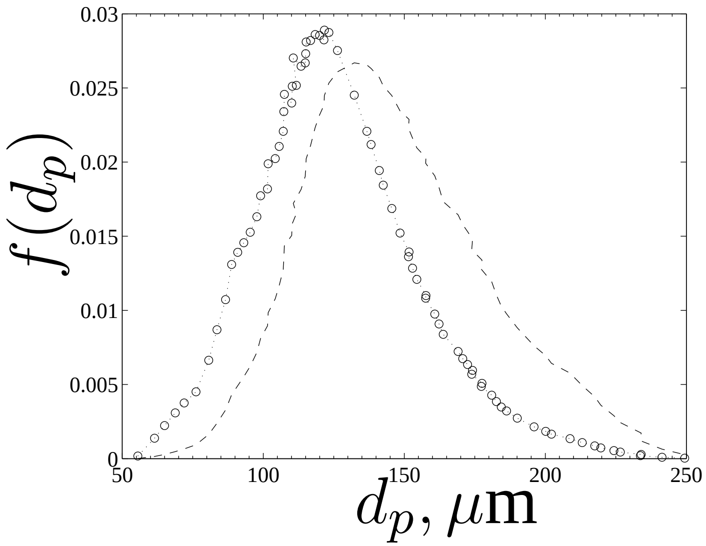

Particle size distribution, $\circ$, number based distribution ; $--$, volume based distribution.

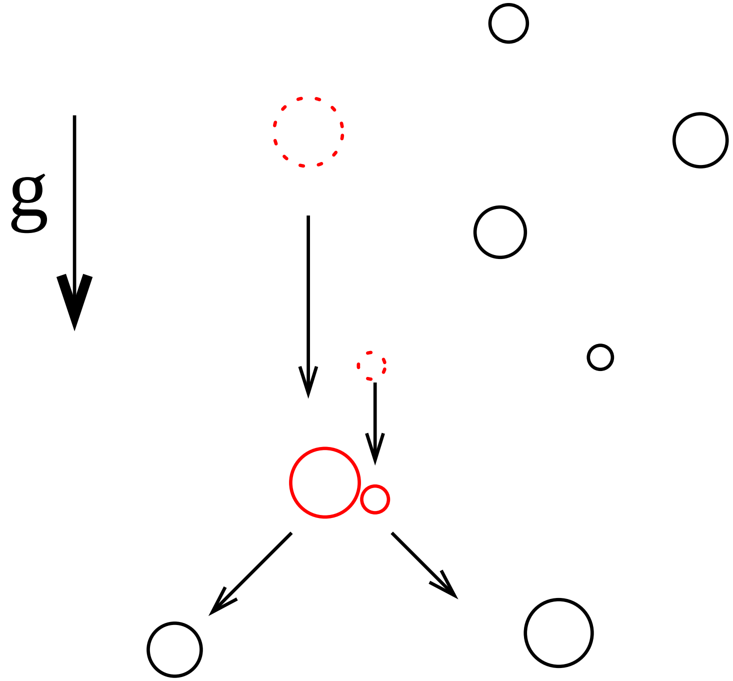

which increases particle fluctuations.

Particle phase — polydispersity:

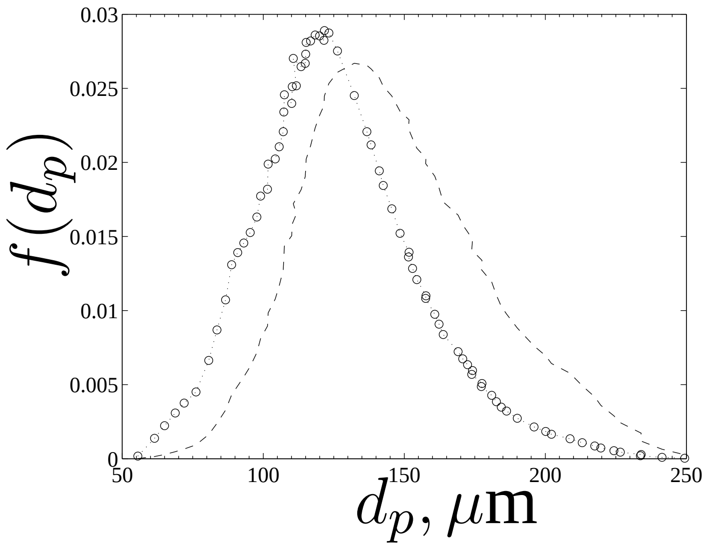

Particle size distribution, ○, number based distribution ; −−, volume based distribution.

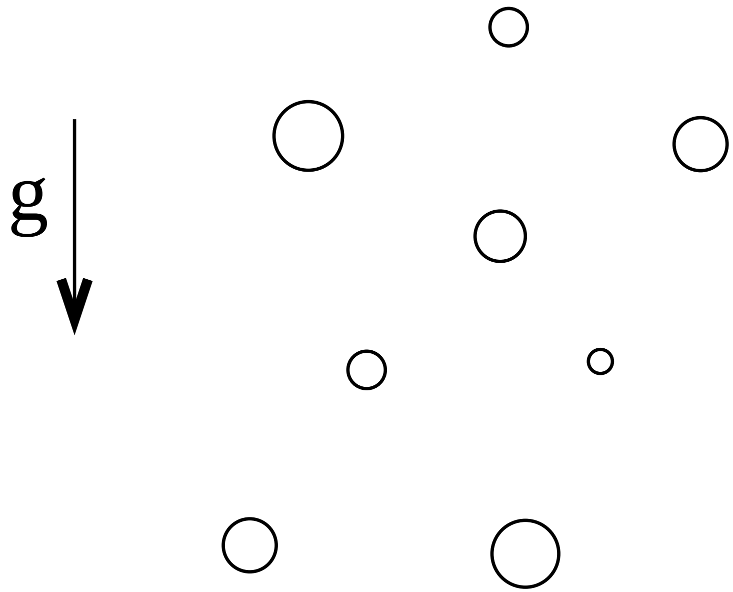

Polydispersity in fluctuating force simulations.

Particle-wall collisions:

- Particle-particle collisions *elastic* — energy dissipation due to viscous drag larger than that due to particle collisions.
- Particle-wall collisions *inelastic*.
- Energy flux to the wall.
- Simple model:
  $v_n' = -e_n v_n$
  $v_t' = e_t v_t$
- Examine effect of coefficient of restitution.

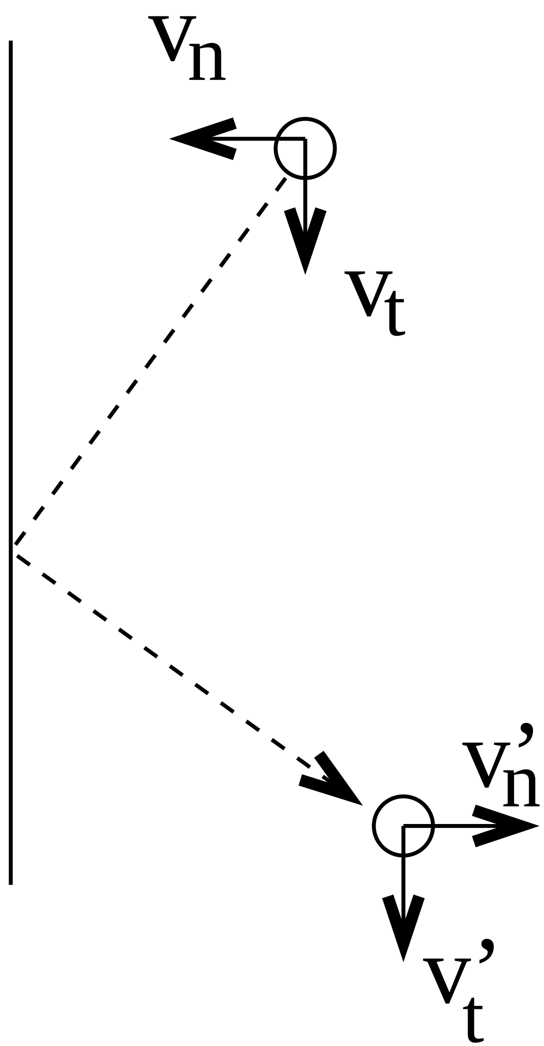

Simulations vs. Experiments:

Low particle loading.
Volume fraction $\phi = 9 \times 10^{-5}$
Mass loading 0.225 kg/kg.

Time scale $\tau_v < \tau_c$.

Simulations vs. Experiments: $(\tau_v < \tau_c)$ $\phi = 9 \times 10^{-4}$

Gas phase:

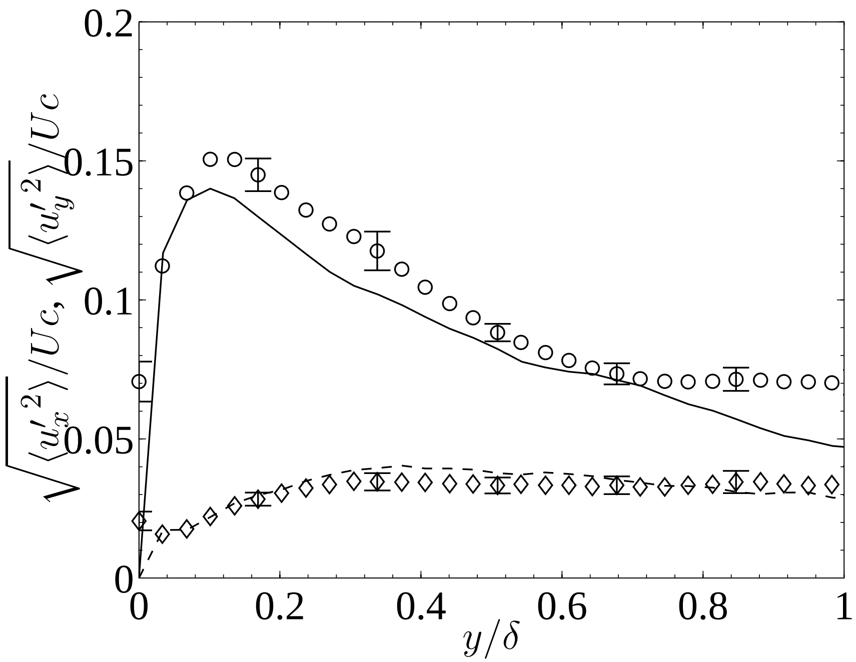

Gas phase turbulence intensities for particle laden and unladen flows

(○) u_{rms}, Particle laden; (◇), v_{rms}, Particle laden; (—) u_{rms}, unladen; (− −) v_{rms}, unladen

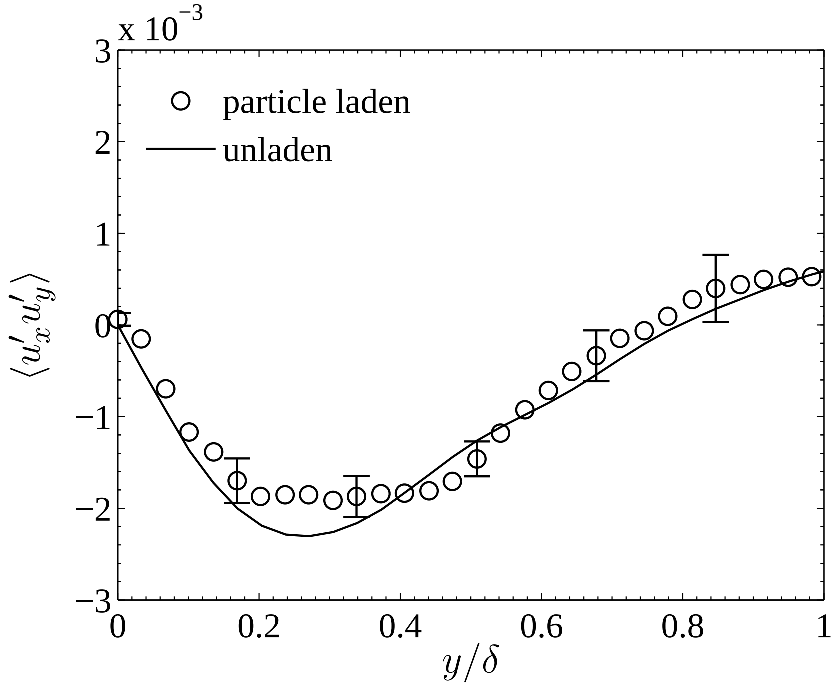

Second moment of gas phase velocity fluctuation for particle laden and unladen flows

Simulations vs. Experiments: $\tau_v < \tau_c$ $\phi = 9 \times 10^{-5}$:

Particle phase:

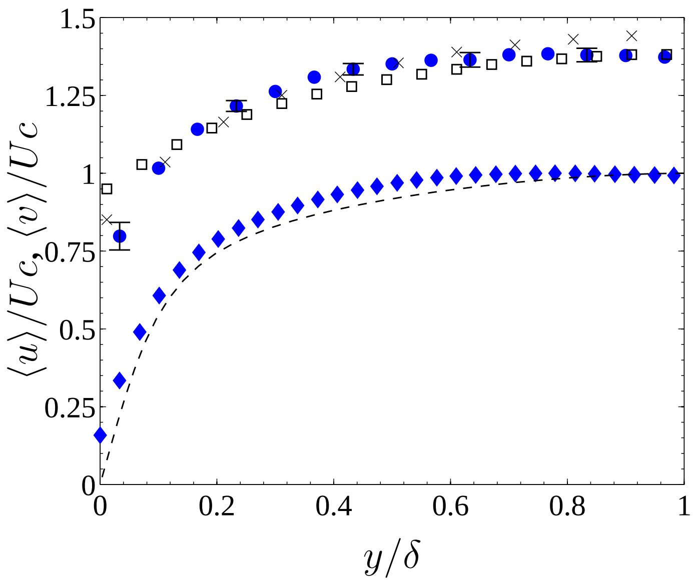

Mean stream-wise velocity of the particle.

($\bullet$), mean particle velocity (V_x); ($\blacklozenge$), mean air velocity (U_x); (— —), U_x, FFS; ($\square$), V_x, $e_n = 1.0$, $e_t = 0.7$; ($\times$), V_x, $e_n = 0.7$, $e_t = 0.7$;

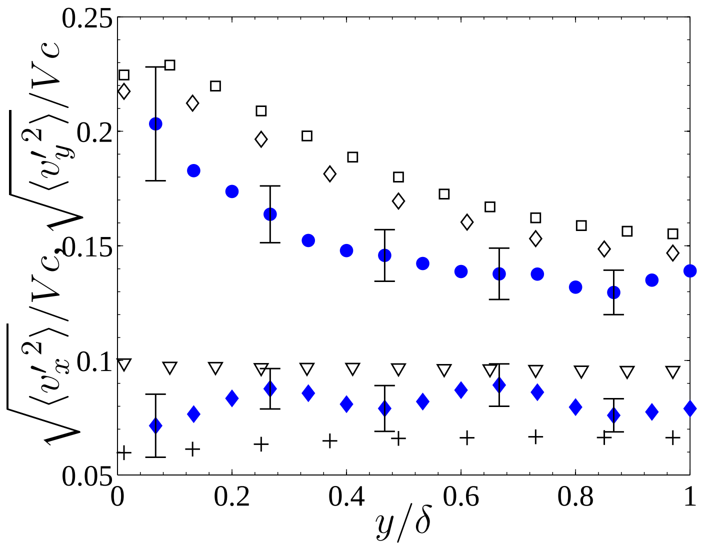

Intensity of particle phase velocity fluctuation

($\bullet$), $\sqrt{\langle {v'_x}^2 \rangle}/Vc$, experiment; ($\blacklozenge$), $\sqrt{\langle {v'_y}^2 \rangle}/Vc$, experiment; ($\square$), $e_n = 1.0$, $e_t = 0.7$; ($\diamond$), $e_n = 0.7$, $e_t = 0.7$; (∇), $e_n = 1.0$, $e_t = 0.7$; ($+$), $e_n = 0.7$, $e_t = 0.7$.

Simulations vs. Experiments: $\tau_v < \tau_c \; \phi = 9 \times 10^{-5}$:

Particle phase:

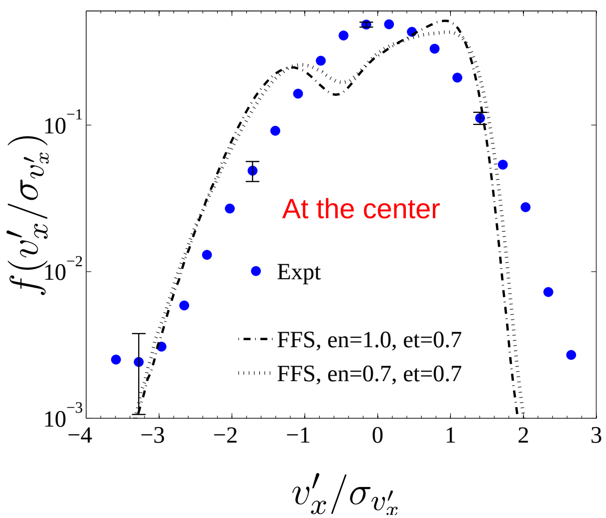

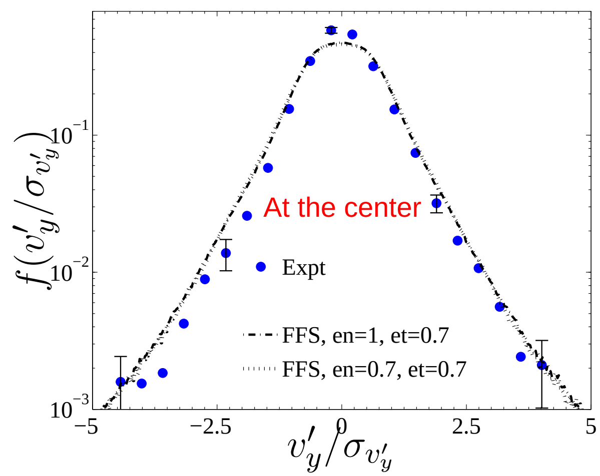

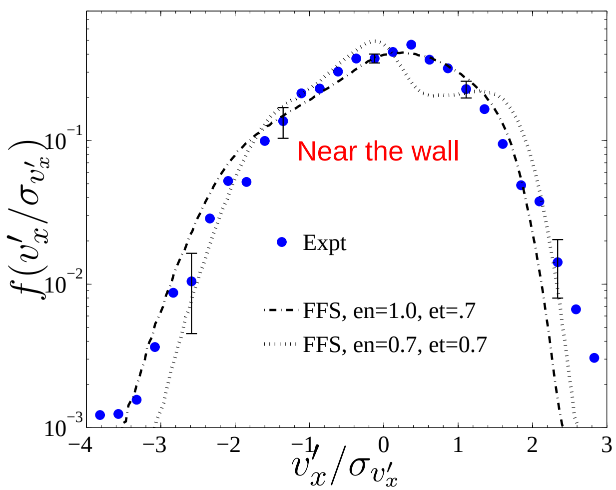

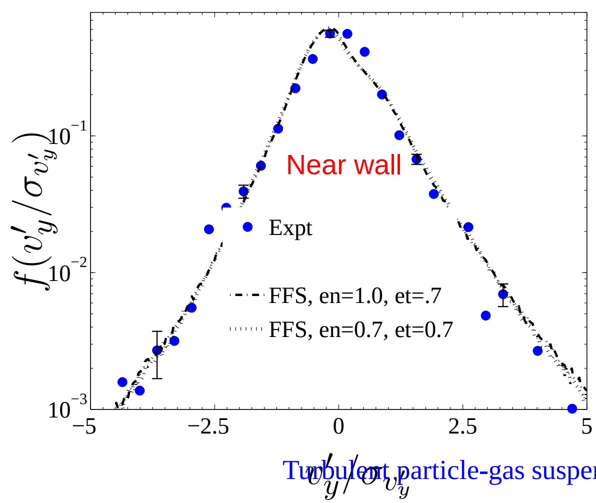

Simulations vs. Experiments:

Moderate particle loading.
Volume fraction $\phi = 7 \times 10^{-4}$
Mass loading 2 kg/kg.

Time scale $\tau_c < \tau_v$.

Simulations vs. Experiments: $\tau_c < \tau_v$ $\phi = 7 \times 10^{-4}$:

Gas phase statistics:

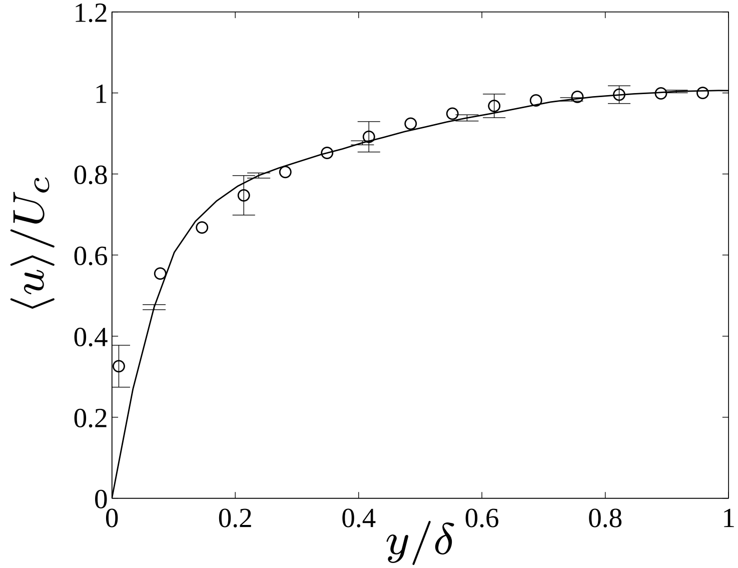

Mean gas velocity for (○)particle laden flow; (—) and unladen flow.

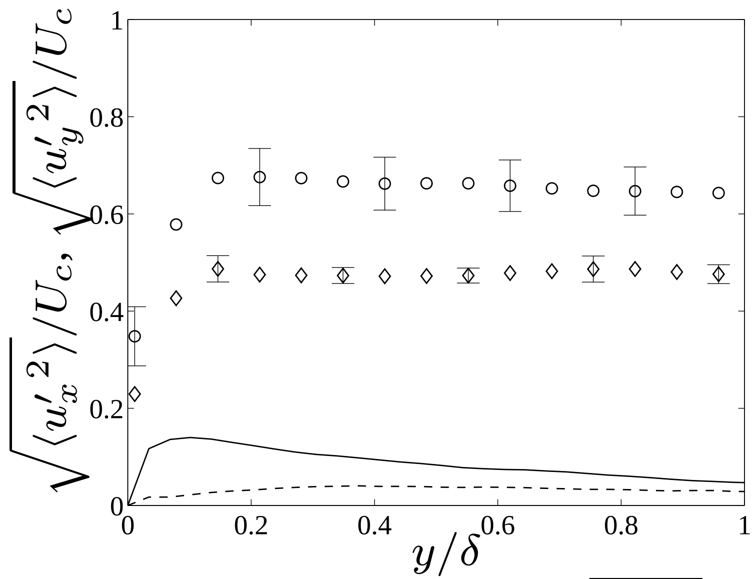

Turbulence intensities for (○), $\sqrt{\langle {u'_x}^2 \rangle}/U_c$, particle laden; (—) $\sqrt{\langle {u'_x}^2 \rangle}/U_c$, unladen; (◇), $\sqrt{\langle {u'_y}^2 \rangle}/U_c$, particle laden; (– –), $\sqrt{\langle {u'_y}^2 \rangle}/U_c$, unladen.

Simulations vs. Experiments: $\tau_c < \tau_v$ $\phi = 7 \times 10^{-4}$:

Gas phase statistics:

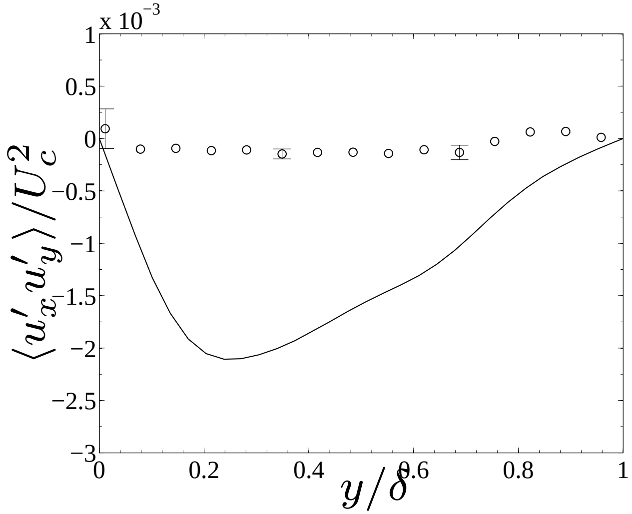

Second moment of the gas phase velocity fluctuation for particle laden and unladen flows. (○), particle laden; (—), unladen flow.

Simulations vs. Experiments: $\tau_c < \tau_v$ $\phi = 7 \times 10^{-4}$:

Particle phase concentration & mean velocity:

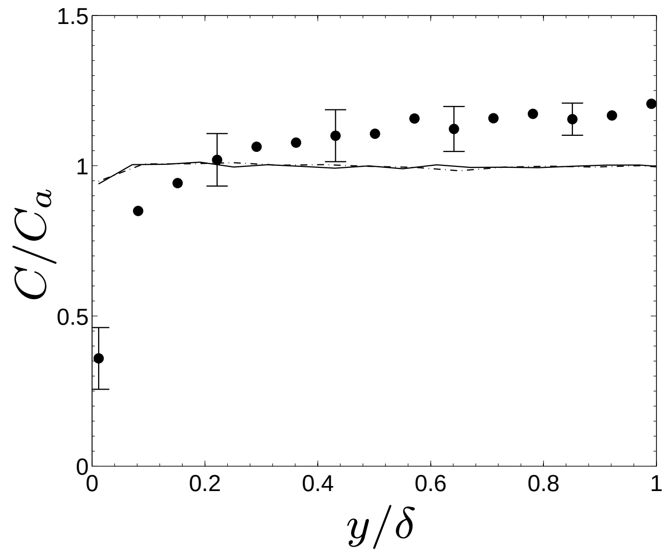

Particle concentration across the channel. ($\bullet$), Experiment; (—), $e_n = e_t = 1.0$, FFS; ($- \cdot -$), $e_n = 1.0, e_t = 0.7$, FFS;

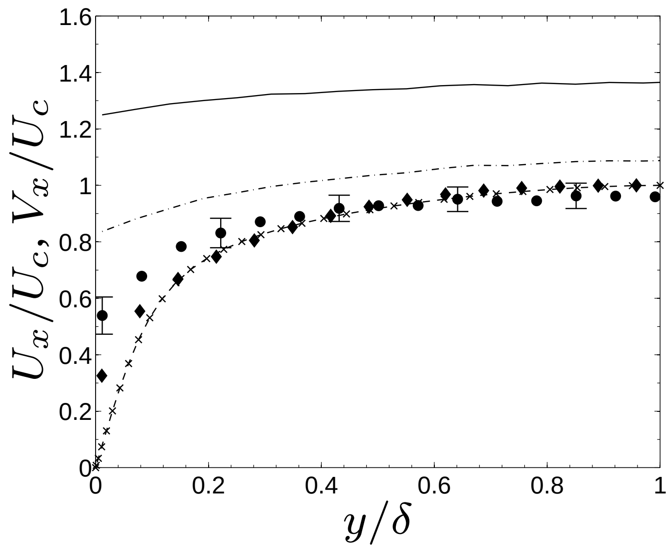

($\bullet$), mean particle velocity (V_x), experiment, ($\blacklozenge$), mean air velocity (U_x), experiment, (—), V_x, $e_n = e_t = 1.0$; ($- \cdot -$), V_x, $e_n = 1.0, e_t = 0.7$.

Simulations vs. Experiments: $\tau_c < \tau_v \; \phi = 7 \times 10^{-4}$:

Particle rms fluctuating velocity:

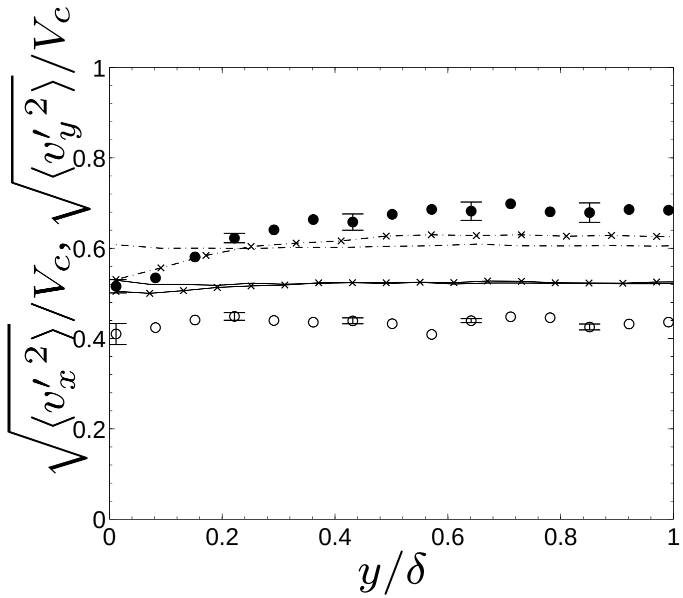

(●), $\sqrt{\langle v_x'^2\rangle}/V_c$, experiment; (○), $\sqrt{\langle v_y'^2\rangle}/V_c$, experiment; (—×), $\sqrt{\langle v_x'^2\rangle}/V_c$, $e_n = e_t = 1.0$, FFS; (—), $\sqrt{\langle v_y'^2\rangle}/V_c$, $e_n = e_t = 1.0$, FFS; (− · −), $\sqrt{\langle v_y'^2\rangle}/V_c$, $e_n = 1.0, e_t = 0.7$, FFS;

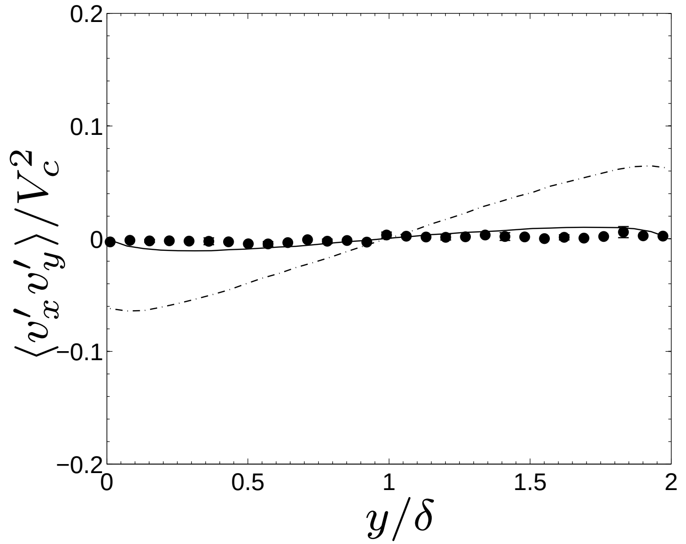

(●), experiment; (—) $e_n = e_t = 1.0$, FFS; (− · −) $e_n = 1, e_t = 0.7$, FFS;

Experiments:

High particle loading.
Volume fraction $\phi = 3.2 \times 10^{-3}$
Mass loading 8 kg/kg.

High particle loading experiments:

Particle Statistics

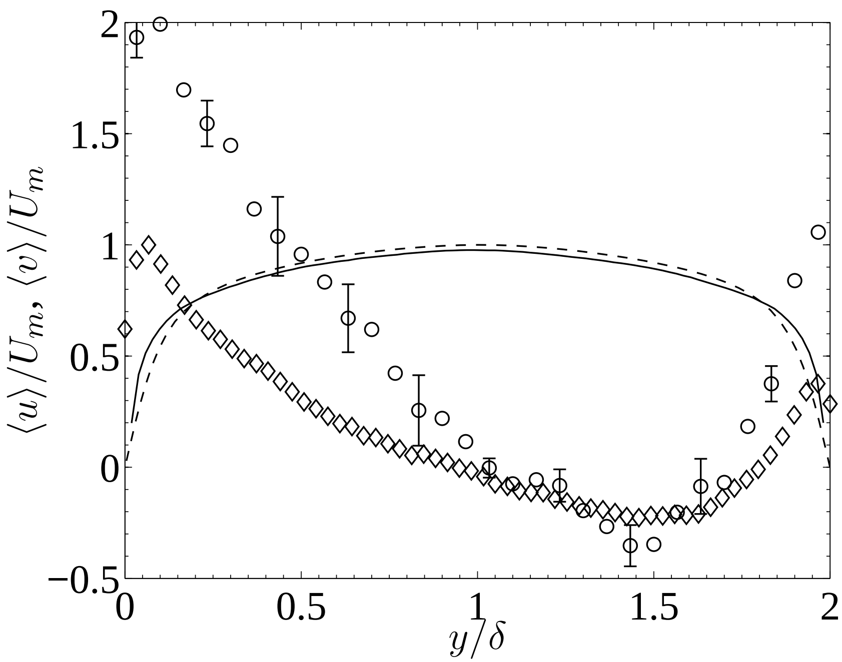

Mean stream-wise velocity of the particle.

(○) Particle velocity, Experiment; (◇) Air velocity, Experiment;

(—) Particle velocity, FFS ; −− Air velocity, FFS

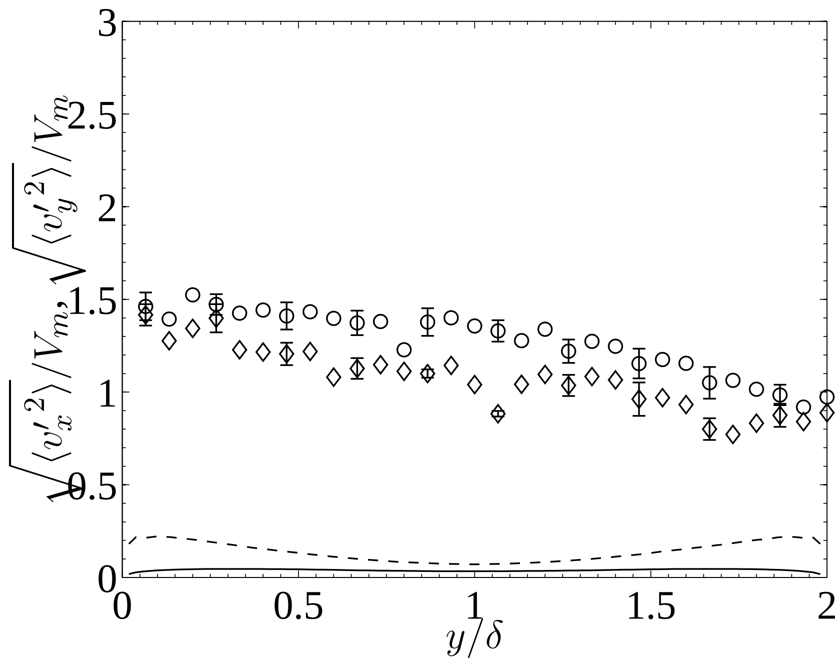

Intensity of particle phase velocity fluctuation

(○) u_{rms}, Experiment; (◇) v_{rms}, Experiment;

−− u_{rms}, FFS; (—) v_{rms}, FFS

High particle loading experiments:

Gas phase Statistics

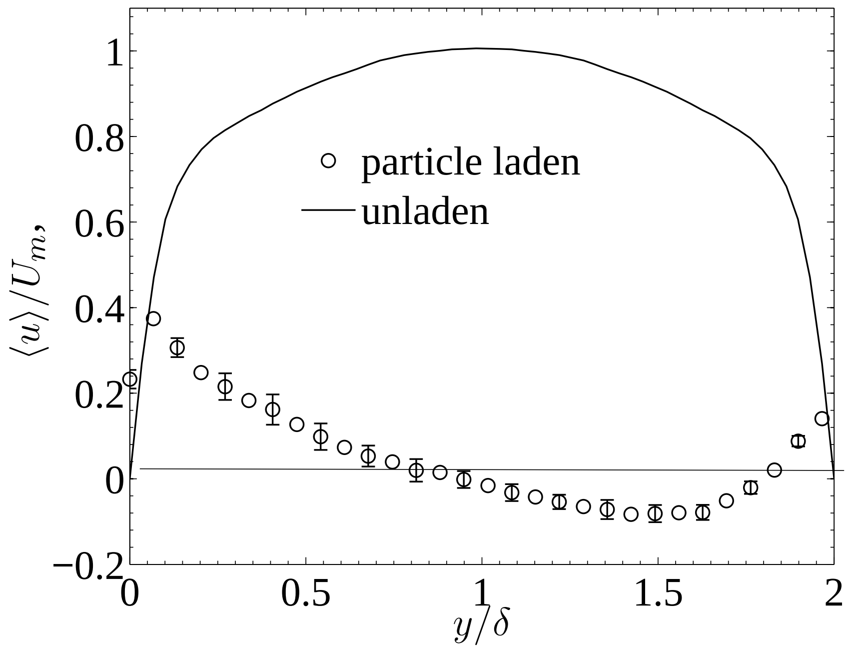

Mean gas velocity for particle laden and unladen flows.

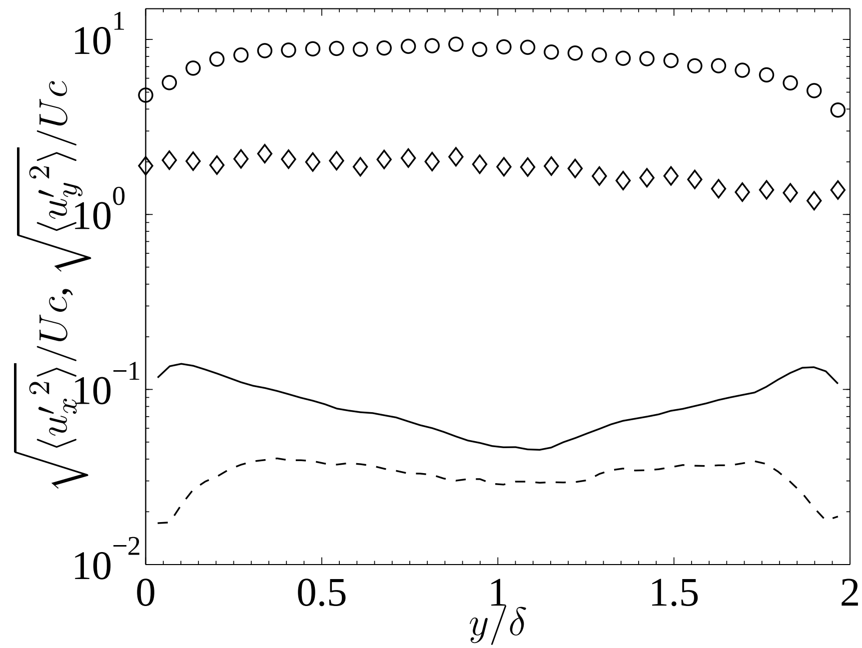

Gas phase turbulence intensities for particle laden and unladen flows. ($\circ$) u_{rms}, Particle laden; ($\diamond$), v_{rms}, Particle laden;

(—) u_{rms}, unladen; (−−) v_{rms}, unladen

Summary

- Low loading solid volume fraction $\phi = 9 \times 10^{-5}$, mass loading = 0.225, $\tau_v < \tau_c$.
  - Experimental results show good agreement with FFS simulation using polydispersed particles.
- Moderate loading solid volume fraction $\phi = 7 \times 10^{-4}$, mass loading = 2, $\tau_c < \tau_v$.
  - Significant turbulence modification.
  - Experimental results show good agreement with FFS simulation using polydispersed particles, depend on particle-wall coefficient of restitution.
- At high solid volume fraction $\phi = 3.2 \times 10^{-3}$, (mass loading about 8), particle and gas velocities are correlated. Random forcing approximation not valid.

Theoretical development: Particle phase.

Kinetic theory for granular flows:

- Velocity distribution $f(\mathbf{x}, \mathbf{v}) d\mathbf{x} d\mathbf{v}$.
- Fluctuating velocity $\mathbf{c} = \mathbf{v} - \mathbf{V}$

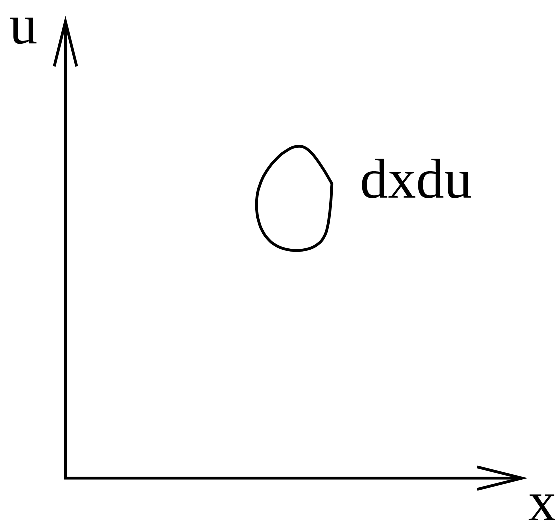

Kinetic theory for granular flows:

Boltzmann eq

$$\frac{\partial(\rho f)}{\partial t} + \frac{\partial(\rho c_i f)}{\partial x_i} + \frac{\partial(\rho a_i f)}{\partial c_i} - \frac{\partial U_i}{\partial x_j}\frac{\partial(\rho c_j f)}{\partial c_i} = \frac{\partial_c(\rho f)}{\partial t}$$

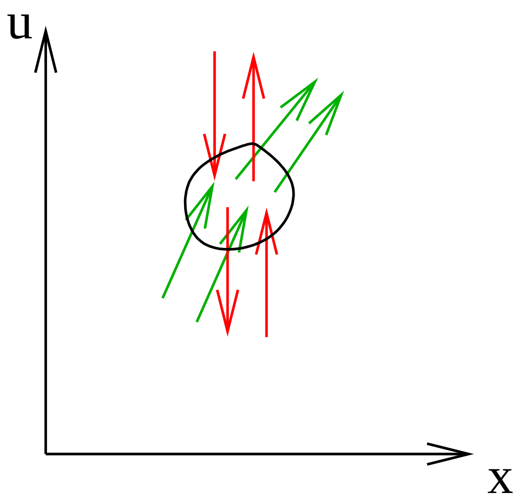

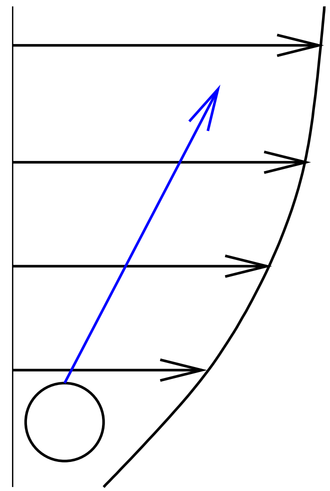

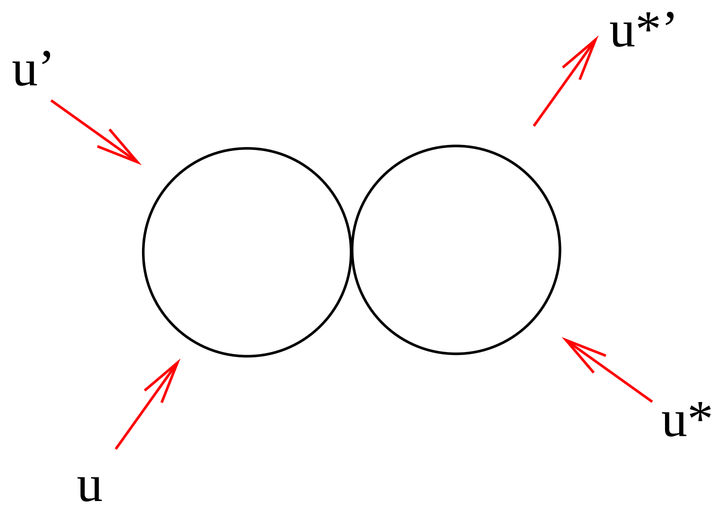

Collision integral:

$$\frac{\partial_c \rho f}{\partial t} = \int_{\mathbf{k}} \int_{\mathbf{c}^*} \left(f(\mathbf{c}') f(\mathbf{c}^{*\prime}) - f(\mathbf{c}) f(\mathbf{c}^*) \right) ((\mathbf{u} - \mathbf{u}^*).\mathbf{k})$$

Turbulent suspensions:

Fokker-Planck-Boltzmann equation:

$$\frac{\partial f}{\partial t} + (\bar{v}_i + v_i')\frac{\partial f}{\partial x_i} - \frac{\partial((v_i' + \bar{v}_i - \bar{u}_i)f)}{\tau_v \partial v_i'} - \frac{\partial U_i}{\partial x_j}\frac{\partial(v_i' f)}{\partial v_j'} - D_{ij}\frac{\partial^2 f(\mathbf{v}')}{\partial v_i' \partial v_j'} = \frac{\partial_c f}{\partial t}$$

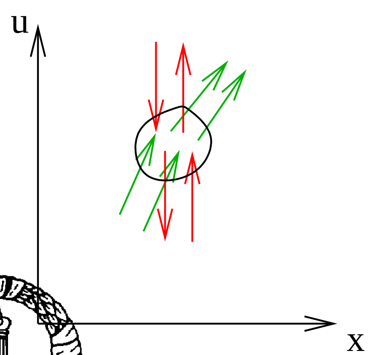

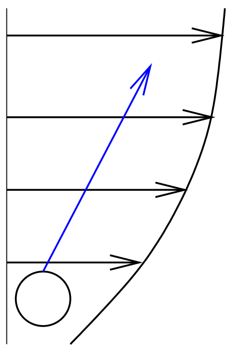

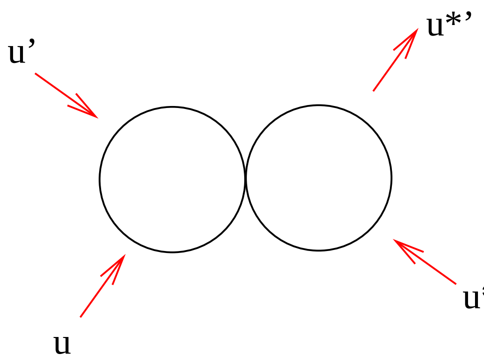

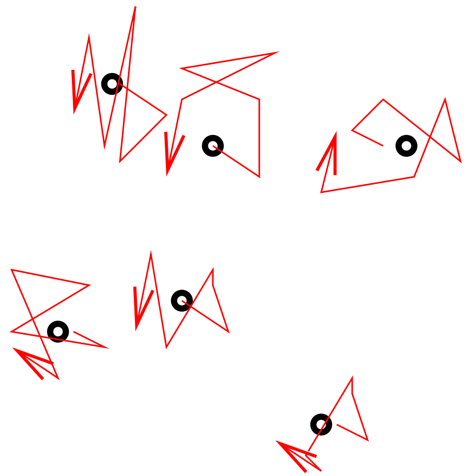

Turbulent suspensions: FPB equation.

$$\frac{\partial f}{\partial t} + (\bar{v}_i + v'_i)\frac{\partial f}{\partial x_i} - \frac{\partial((v'_i + \bar{v}_i - \bar{u}_i)f)}{\tau_v \partial v'_i}$$
$$- \frac{\partial U_i}{\partial x_j}\frac{\partial (v'_i f)}{\partial v'_j} - D_{ij}\frac{\partial^2 f(\mathbf{v}')}{\partial v'_i \partial v'_j} = \frac{\partial_c f}{\partial t}$$

Equilibrium (no gradients) $\frac{\partial_c f}{\partial t} = 0$
Solution — Maxwell-Boltzmann distribution
$f_0 = (2\pi T/m)^{-3/2} \exp\left(-m v_i'^2/2T\right)$

Temperature determined by balance between source due to shear, collisions, turbulent fluctuations and dissipation due to drag.

Turbulent suspensions: FPB equation.

$$\frac{\partial f}{\partial t} + (\bar{v}_i + v'_i)\frac{\partial f}{\partial x_i} - \frac{\partial((v'_i + \bar{v}_i - \bar{u}_i)f)}{\tau_v \partial v'_i}$$

$$- \frac{\partial U_i}{\partial x_j}\frac{\partial(v'_i f)}{\partial v'_j} - D_{ij}\frac{\partial^2 f(\mathbf{v}')}{\partial v'_i \partial v'_j} = \frac{\partial_c f}{\partial t}$$

Anisotropic Brownian motion with drag:

$$-\frac{\partial(v'_i f)}{\tau_v \partial v'_i} - D_{ij}\frac{\partial^2 f(\mathbf{v}')}{\partial v'_i \partial v'_j} = 0$$

Solution — Anisotropic Gaussian distribution:

$$f_0 = (2\pi \mathbf{Det}\mathbf{T})^{-3/2} \exp\left(-(1/2) m v'_i T^{-1}_{ij} v'_j\right)$$

Turbulent suspensions: FPB equation

Conservation equations: Chapman-Enskog procedure.

$$f = f_0(1 + \epsilon\phi_1 + \epsilon^2\phi_2 + \ldots)$$

Multiply FPB equation by mass, momentum, energy, and integrate over velocities to obtain conservation equations.
Mass conservation:

$$\frac{\partial\rho}{\partial t} + \nabla.(\rho\mathbf{V}) = 0$$

Conservation equations:

Momentum conservation:

$$\rho \frac{DV}{Dt} = \nabla.\sigma - \frac{\rho(\mathbf{U} - \mathbf{V})}{\tau_v}$$

$$\sigma = -p\mathbf{I} + \mu(\nabla\mathbf{V} + (\nabla\mathbf{V})^T) + (\mu_b - 2/3\mu)\mathbf{I}\nabla.\mathbf{V} - \mathbf{E}$$

$$E_{ij} = \frac{5(D_{ij} - (\delta_{ij}/3)D_{kk})}{8\sqrt{\pi}T^{1/2}}$$

Conservation equations:

Energy conservation:

$$\rho C_v \frac{DT}{Dt} = -p\nabla.\mathbf{V} + \rho D_{ii} - \rho E_{ik} S_{ki} + 2\mu S_{ik} S_{ki}$$
$$+\mu_b(\nabla.\mathbf{V})^2 - 2\rho C_v T/\tau_v - \nabla.\mathbf{q}$$

$$\mathbf{q} = -K\nabla T$$

Consequences of fluctuating force:

Fluidised bed:

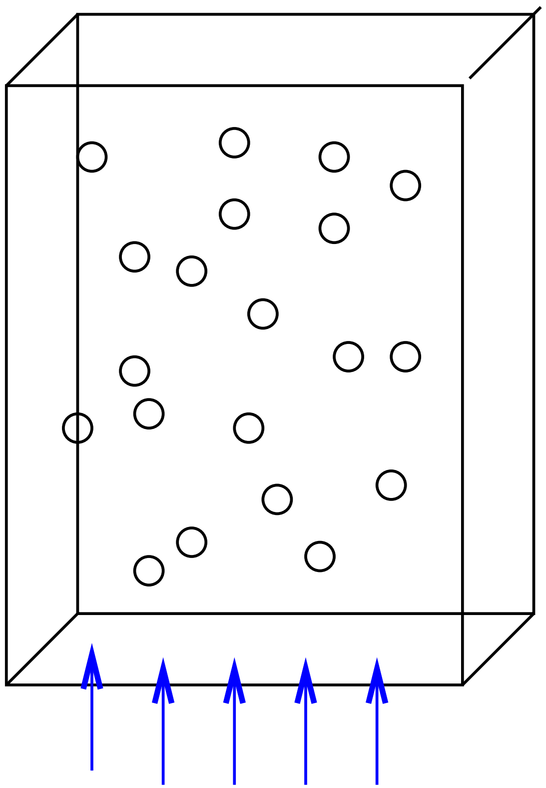

- Two-fluid models, in which the particle drag depends on local concentration, predict that the uniformly fluidised state is always unstable (Jackson 1966).
- Fluctuating force stabilises uniform state due to homogenisation of fluctuations.

Consequences of fluctuating force:

Turbophoresis:

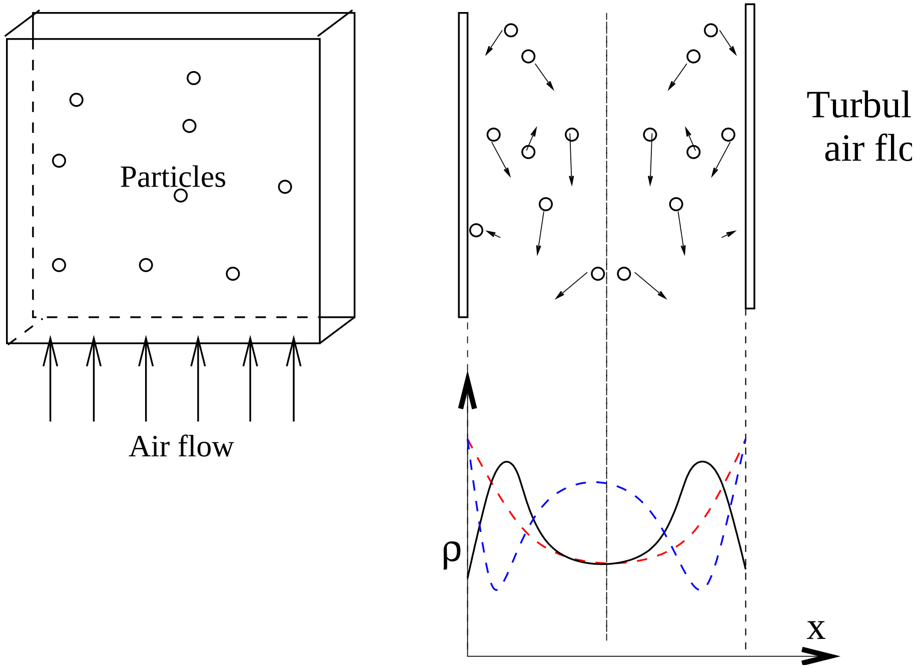

- Non-monotonic variation of concentration across channel.
- Correlates with the variation of the fluctuating force amplitude.

Summary

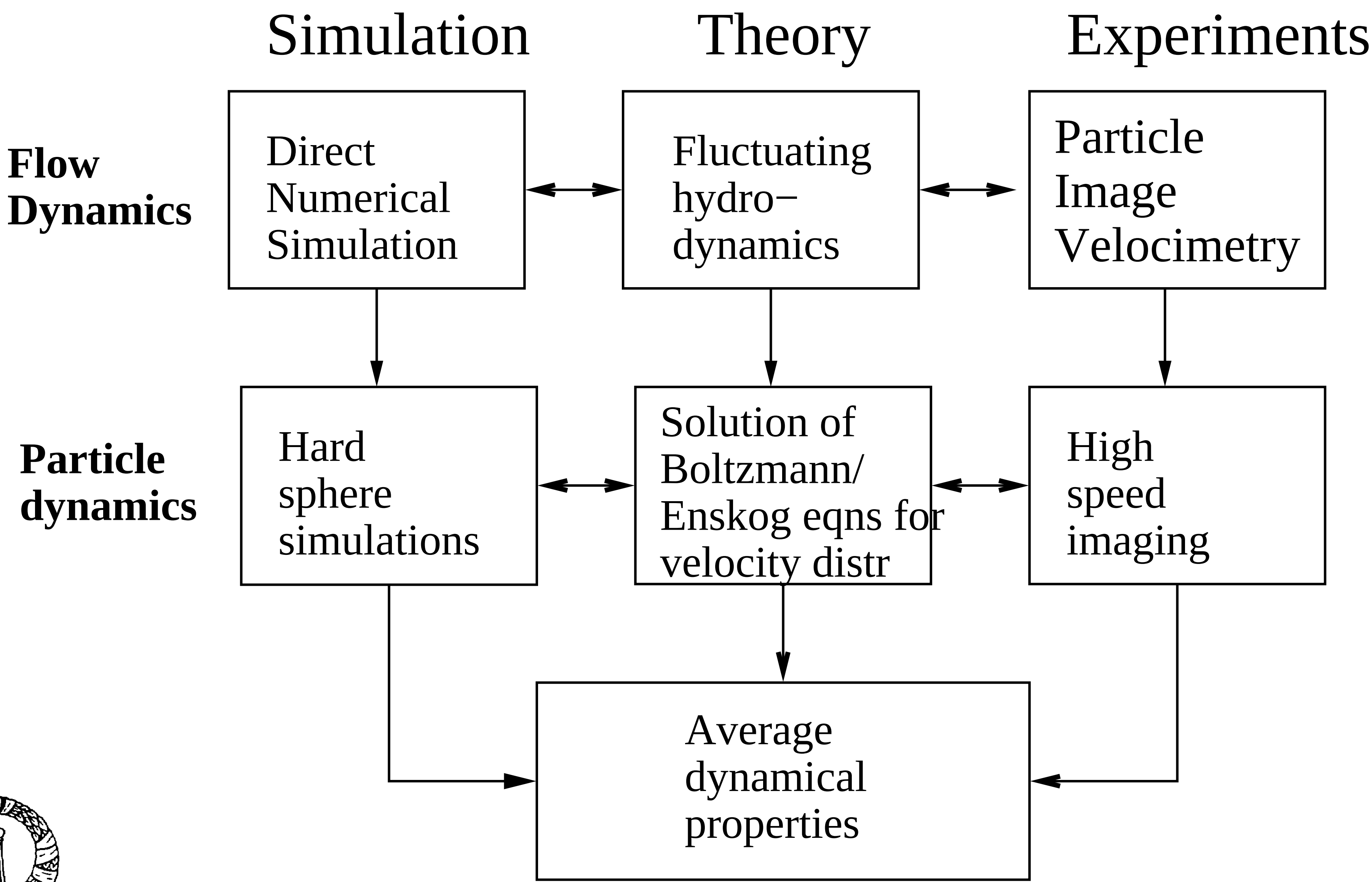
Simulation
Theory
Experiments
Flow Dynamics
Particle dynamics
Direct Numerical Simulation
Fluctuating hydro−dynamics
Particle Image Velocimetry
Hard sphere simulations
Solution of Boltzmann/ Enskog eqns for velocity distr
High speed imaging
Average dynamical properties

Future work:

- Reverse coupling — effect of particle force on fluid turbulence.
- Incorporate coupling in particle/fluid fluctuations into continuum models.
- Transport rates.

Thank You